Dynamic bond percolation theory for diffusion of interacting particles: Tracer diffusion in a binary mixture lattice gas

Rony Granek and Abraham Nitzan
School of Chemistry, Sackler Faculty of Exact Sciences, Tel-Aviv University, Tel-Aviv 69978, Israel

(Received 8 January 1990; accepted 6 June 1990)

Dynamic percolation theory is used to obtain the tracer diffusion coefficient in binary mixtures of "noninteracting" lattice gas (with only the blocking interactions, i.e., double occupancy of a lattice site is forbidden) within the effective medium approximation (EMA). Our approach is based on regarding the background particles as a changing random environment. The result is expressed in terms of two fluctuation time parameters which we attempt to determine self-consistently. We compare two possible choices for these parameters which are consistent with our former results for the single component system. The resulting tracer diffusion coefficient for both choices compares well with numerical simulations whenever single bond EMA is expected to be reliable. Comparison is also made with the theoretical results of Sato and Kikuchi [Phys. Rev. B **28**, 648 (1983)] and discrepancies between both theories are discussed.

I. INTRODUCTION

Diffusion of independent particles in static percolating networks has been thoroughly investigated in the past two decades.[1-7] However, in reality the diffusing particles interact among themselves, thus limiting the validity of these studies to extremely low concentrations. A more general situation is that of a binary mixture of diffusing particles. The latter case reduces to the former when particles of one kind are infinitely slow relative to the other kind. From the experimental point of view these situations are encountered in mixed alloys,[8(a)] mixed ionic conductors,[8(b)] reacting and nonreacting adsorbate mixtures on solid surfaces,[8(c)] interdiffusion in mixed polymer melts,[8(d)] and in many other systems.

There is a substantial amount of analytical and simulation work[9-16] on particle motion in the so-called "noninteracting" lattice gas (NILG) where only blocking interactions are taken into account (namely, double occupancy of a site is forbidden). However, whereas some simulation work on NILG mixtures have been done,[17-23] only a few analytical studies (of NILG mixtures) have been described.[24-28] With the exception of the theory of Sato and Kikuchi,[25] these theories are limited to jump rate ratios $\gamma = \Gamma_A/\Gamma_B$ between the components which are not too small (or too large), and, in particular, fail to predict the percolation threshold in the $\gamma \to 0, \infty$ limits: in the binary mixture lattice gas (LG), when one component (say A) is static relative to the other one (B), the tracer diffusion coefficient of the fast particles B should vanish at and below the percolation threshold created by the A particles. This situation differs from that of a single particle diffusion in a static disordered lattice since the B particles also interact among themselves.

Recently,[16] we have successfully applied dynamic bond percolation (DBP) theory[29-42] for tracer diffusion in a single component lattice gas. A similar approach has been discussed by Hilfer and Orbach.[42(b)] The approach was based on the observation that the background particles can be viewed as a changing random environment for the tracer. We have shown[16] (for self-diffusion, i.e., for the case of identical tracer and background particles) that this theory yields a fairly good approximation for the tracer diffusion coefficient in the whole concentration regime. For the small vacancy concentration limit our theory yields standard approximate results, originally derived by Kikuchi.[10] For different tracer (B) and background (A) particles the standard effective medium approximatioin (EMA) result for a single particle moving in a static random bond network and the mean-field result for the tracer diffusion coefficient were obtained in the $\gamma \to 0$ and $\gamma \to \infty$ limits, respectively.

In this paper we generalize our method for the case of tracer diffusion in multicomponent "noninteracting" lattice-gas (blocking interactions only) mixtures. In this model, each particle of component i has a bare jump rate Γ_i, from one site to a *vacant* nearest-neighbor site, independent of its environment. To find the tracer diffusion coefficient, we make use of the EMA for the many bond states dynamic percolation theory, previously derived by us[38] as an extension of the EMA theory of Harrison and Zwanzig (HZ).[37]

We study in detail the binary mixture case, which is relevant for binary alloys, diffusion of co-adsorbed molecules on surfaces and (with Coulombic interaction neglected) for ion migration in solids. A tracer O particle is assumed to hop among A and B particles. An explicit expression for the tracer diffusion coefficient is obtained in terms of the concentrations c_A and c_B, the hopping rates Γ_0, Γ_A, and Γ_B (Γ_0 is the tracer hopping rate), and two (initially unknown) local fluctuation times τ_A and τ_B. For the latter quantities we use two possible ansatzs, one—based on the mean-field approximation—takes $\tau_i = (Z-1)\Gamma_i$ (Z is the number of nearest neighbors), while the other relates the times τ_i to the chemical diffusion coefficients of the system. The result is analyzed in detail in the limit of one static component $\gamma = \Gamma_A/\Gamma_B \to 0$ (or, equivalently, $\gamma \to \infty$) and also in the limit of small vacancy concentration $c_V \to 0$ ($c_V = 1 - c = 1 - c_A - c_B$). Special attention is given to the cases $\Gamma_0 = \Gamma_A$ and $\Gamma_0 = \Gamma_B$ which yield the results for the tracer diffusion coefficients of A and B components, respectively.

Our approximate results are compared to results of nu-

 0021-9606/90/205918-17$03.00

merical simulations for both the static ($\gamma = 0$) and dynamic ($\gamma > 0$) cases. Good agreement is found for both choices of fluctuation times in all situations where single bond dynamics (neglect of dynamic and static correlations) and single bond EMA are expected to be valid.

This paper is organized as follows. The multicomponent system is studied generally in Sec. II. An explicit solution for the binary system is obtained in Sec. III. In Sec. IV we discuss the fluctuation times needed for the calculation and express them in terms of the bare hopping rates Γ_i, the number of nearest neighbors Z, and (for one of the two ansatzs) in terms of the chemical diffusion coefficients. The limit of one static component and the small vacancy concentration limit are investigated in Secs. V and VI. In Sec. VII we obtain an approximate expression for the chemical diffusion coefficients of the system, needed for the calculation of the local fluctuation times. We conclude in Sec. VIII by presenting some numerical results and comparing them to results of numerical simulations.

II. THE MULTICOMPONENT MIXTURE

Consider an n component (not counting vacancies) "noninteracting" lattice gas (blocking interactions only) whose constituents are $A_1, A_2, A_3, ..., A_n$ with corresponding elementary jump rates $\Gamma_1, \Gamma_2, \Gamma_3, ..., \Gamma_n$. We consider the diffusion of a tracer O particle with an elementary jump rate Γ_0 embedded in this LG. Focussing on a nearest-neighbor (NN) bond to the tracer O particle we can define a stochastic state variable ξ for this bond which is related to the kind of particle that occupies the corresponding NN site to the tracer, either $A_1, A_2, A_3, ..., A_n$ or neither of them—V (for vacancy). Thus, ξ can take the symbolic "values" $\xi = A_1, A_2, A_3, ..., A_n, V$. The stochastic (dimensionless) jump rate of the tracer particle to that NN site is given by the function $\sigma(\xi)$ defined as

$$\sigma(\xi) = \left\{ \begin{array}{ll} 1 & \text{if } \xi = V \\ 0 & \text{if } \xi = A_1,...,A_n \end{array} \right\}. \tag{2.1}$$

Thus each bond is associated with only two basic rates, 0 and 1, however $\sigma(\xi) = 0$ corresponds to many states of a bond. The transition between the bond states is *assumed* to be described by a characteristic *Markovian* rate equation

$$\frac{\partial}{\partial t} f_\alpha(\xi,t) = \sum_{\xi'} \Omega_\alpha(\xi,\xi') f_\alpha(\xi',t), \tag{2.2}$$

where $f_\alpha(\xi,t)$ is the probability that bond α is in state ξ at time t and $\Omega_\alpha(\xi,\xi')$ is a characteristic rate matrix. Its elements have to be found from the lattice-gas dynamics itself. $\Omega_\alpha(\xi,\xi')(\xi \neq \xi')$ is the transition rate constant to go from bond state ξ' to bond state ξ while $\Omega_\alpha(\xi,\xi) = -\sum_{\xi' \neq \xi} \Omega_\alpha(\xi',\xi)$ is the rate constant out of state ξ. It is important to note that this Markovian assumption is an approximation; the precise dynamics is more likely to be non-Markovian.

The elements $\Omega(\xi,\xi')$ are determined in the following way: First, we do not allow a direct exchange between the particles. This is impossible because of the blocking interactions. Second, we choose them to obey detailed balance conditions. Thus, given the concentrations $\{c_i\}$ of the $\{A_i\}$ $(i = 1,...,n)$ components, the matrix elements $\Omega(\xi,\xi')$ are given by

$$\Omega(A_i,V) = c_i/\tau_i,$$
$$\Omega(V,A_i) = c_V/\tau_i, \quad \Omega(A_i,A_j) = -(c_V/\tau_i)\delta_{ij},$$

and

$$\Omega(V,V) = -\sum_i c_i/\tau_i, \tag{2.3}$$

where $c_V = 1 - c$, with $c = \Sigma_i c_i$ being the total concentration of particles, is the vacancy concentration. The fluctuation time parameters $\{\tau_i\}$ $(i = 1,...,n)$ are, in principle, functions of the jump rates Γ_i and the concentrations $\{c_i\}$. The simplest choice for these parameters is obtained from the following mean-field approach, previously described in Ref. 16 for the one component system. First, we find the mean-field jump rate of an i type particle from a site which is NN to our tracer particle. This rate is $c_V(Z-1)\Gamma_i$, where $Z-1$ instead of Z appears because the tracer site is excluded (Z is the coordination number of the lattice). Comparing these to the corresponding rate implied by Eqs. (2.2) and (2.3), c_V/τ_i, we find that

$$\tau_i^{-1} = (Z-1)\Gamma_i, \quad i = 1,...,A_n. \tag{2.4}$$

A more general discussion of the times τ_i is given in Sec. IV. In the following results we do not use explicitly Eq. (2.4).

Following our previous treatment for one component lattice gas,[16] which makes use of the HZ formalism,[37] the tracer random walk is described by an approximate stochastic master equation for the walker probability $P_i(t)$ to be at site i at time t

$$\frac{d}{dt} P_i(t) = \Gamma_0 \sum_{j \in \{i\}} \sigma[\xi_{ij}(t)][P_j(t) - P_i(t)], \tag{2.5}$$

where $\{i\}$ denotes the group of sites nearest neighbors to i. Our aim is to average over Eq. (2.5) in conjunction with Eq. (2.2). This generally leads to the effective medium equation

$$\frac{d}{dt}\langle P_i(t)\rangle = \Gamma_0 \sum_{j \in \{i\}} \times \int_0^t dt' \, \tilde{\psi}(t-t')[\langle P_j(t')\rangle - \langle P_i(t')\rangle] \tag{2.6}$$

and the problem is to determine the effective rate (memory kernel) $\tilde{\psi}(t)$. A solution for this problem has been obtained in the effective medium approximation (EMA) and is given in detail in Appendix A and in Ref. 38. The result is that the frequency-dependent dimensionless effective jump rate $\psi(\omega)$, the Fourier–Laplace transform of $\tilde{\psi}(t)$, is determined from the requirement that the following set of $n+1$ linear equations should have a nontrivial solution, namely, that the determinant of coefficients of the $\mathbf{Q}_\xi$ ($\mathbf{Q}_\xi$ are vectors in the site space) vanishes:

$$\sum_\xi [\sigma(\xi) - \psi(\omega)]\mathbf{Q}_\xi = 0 \tag{2.7}$$

and

$$\sum_\xi M_\xi^{(l)}(1 + h_l[\sigma(\xi) - \psi(\omega)])\mathbf{Q}_\xi = 0,$$
$$l = 1,...,n. \tag{2.8}$$

Here, $M_{\xi}^{(l)}$ $(l=1,\ldots,n)$ are elements of the left eigenvectors of the transition matrix Ω corresponding to nonzero eigenvalue λ_l, namely,

$$\sum_{\xi'} M_{\xi'}^{(l)}\Omega(\xi',\xi) = -\lambda_l M_{\xi}^{(l)}, \quad \lambda_l > 0; \tag{2.9}$$

the h_l and ϵ_l are given by

$$h_l = \frac{p_c}{\psi}(1-\epsilon_l g(\epsilon_l)), \tag{2.10}$$

where $g(\epsilon)$ is the lattice Green's function at the origin (see Refs. 3–6 and 48 and Appendix E for explicit expressions),

$$\epsilon_l = \frac{i\omega+\lambda_l}{\Gamma_0\psi} \tag{2.11}$$

with Γ_0 being the bare jump rate of the tracer particle O; and where

$$p_c = 2/Z \tag{2.12}$$

is the EMA percolation threshold. Thus, with the elements of the matrix Ω known, Eqs. (2.6)–(2.12) provide a complete EMA solution for the tracer diffusion coefficient in the form (for simple cubic lattices)

$$D_{to}(\omega) = \Gamma_0\psi(\omega)a^2, \tag{2.13}$$

where a is the lattice constant. In the rest of this work we use $a=1$.

In Sec. III we apply the above formalism to the case of binary mixture ($n=2$) and solve explicitly for the tracer diffusion coefficient.

III. THE BINARY MIXTURE

Here we consider a mixture of two types of particles, A and B, with jump rates Γ_A and Γ_B, respectively. Thus, the bond state variable ξ can take the values A, B, or V. The dynamical matrix Ω is therefore 3×3. The elements of Ω are given by Eq. (2.3). Thus, with the concentrations of the two components denoted by c_A and c_B and the (yet undetermined) fluctuation times denoted by τ_A and τ_B, the bond state dynamics is described by

$$\frac{\partial}{\partial t}\begin{pmatrix} f(A,t) \\ f(V,t) \\ f(B,t)\end{pmatrix} = \begin{pmatrix} -c_V/\tau_A & c_A/\tau_A & 0 \\ c_V/\tau_A & -(c_A/\tau_A + c_B/\tau_B) & c_V/\tau_B \\ 0 & c_B/\tau_B & -c_V/\tau_B\end{pmatrix} \times \begin{pmatrix} f(A,t) \\ f(V,t) \\ f(B,t)\end{pmatrix}, \tag{3.1}$$

where $c = c_A + c_B$ is the total concentration of particles and $c_V = 1-c$ is the vacancy concentration.

Following the formalism described in Sec. II, the two nonzero eigenvalues of the matrix Ω are

$$\lambda_{\pm} = \frac{1}{2}\left\{\frac{1-c_A}{\tau_B} + \frac{1-c_B}{\tau_A} \pm \sqrt{\left(\frac{1-c_A}{\tau_B}+\frac{1-c_B}{\tau_A}\right)^2 - \frac{4c_V}{\tau_A\tau_B}}\right\}. \tag{3.2}$$

The associated left eigenvectors $\mathbf{m}_{\pm} = (M_A^{(\pm)}, M_V^{(\pm)}, M_B^{(\pm)})$, corresponding to $\lambda_{\pm}$, are

$$\mathbf{m}_{\pm} = \left(c_V,\ c_V - \tau_A\lambda_{\pm},\ c_V\frac{c_V-\tau_A\lambda_{\pm}}{c_V-\tau_B\lambda_{\pm}}\right). \tag{3.3}$$

Obviously, these eigenvectors are determined only up to a constant. When $\tau_A=\tau_B\equiv\tau$ one has, from Eq. (3.2), $\lambda_+ = 1/\tau$ and $\lambda_- = c_V/\tau$. Thus, for $\mathbf{m}_-$ given by (3.3) both the numerator and denominator of $M_B^{(-)}$ vanish and this term approaches a finite limit

$$M_B^{(-)} = -c_V\frac{c_A}{c_B}, \quad \tau_A=\tau_B \tag{3.4}$$

(see Appendix B).

The fact that in the limit $\tau_A=\tau_B\equiv\tau$, λ_+ becomes the density relaxation rate τ^{-1} is significant. If we define the bond availability probability $\phi(\sigma,t)$ (i.e., the probability to have a bond transition rate σ at time t) by $\phi(0,t) = f(A,t) + f(B,t)$ and $\phi(1,t) = f(V,t)$ we get from Eq. (3.1) the following Markovian equation for ϕ

$$\frac{\partial}{\partial t}\begin{pmatrix}\phi(0,t)\\ \phi(1,t)\end{pmatrix} = \begin{pmatrix} -(1-c)/\tau & c/\tau \\ (1-c)/\tau & -c/\tau\end{pmatrix}\begin{pmatrix}\phi(0,t)\\ \phi(1,t)\end{pmatrix}. \tag{3.5}$$

This equation was shown to be valid,[16] within the mean-field approximation, in the single component NILG with τ given by $\tau^{-1} = (Z-1)\Gamma$. This means that in order to be consistent with our former results[16] in the one component case $\Gamma_A=\Gamma_B\equiv\Gamma$, we must use in this limit $\tau_A=\tau_B=[(Z-1)\Gamma]^{-1}$ for any composition and total concentration.

From Eqs. (2.7) and (2.8), the effective hopping rate $\psi(\omega)$ in the single bond EMA is determined from the requirement

$$\det\begin{bmatrix} -\psi & 1-\psi & -\psi \\ (1-\psi h_+)c_V & [1+h_+(1-\psi)]K_+ & (1-\psi h_+)c_V F_+ \\ (1-\psi h_-)c_V & [1+h_-(1-\psi)]K_- & (1-\psi h_-)c_V F_-\end{bmatrix} = 0, \tag{3.6}$$

where

$$K_{\pm} = c_V - \tau_A\lambda_{\pm}, \tag{3.7a}$$

$$F_{\pm} = \frac{K_{\pm}}{c_V-\tau_B\lambda_{\pm}}. \tag{3.7b}$$

Equation (3.6) may be solved for the EMA effective hopping rate ψ ($\equiv\psi_0$) of the tracer particle. The solution is facilitated by using the identity

$$K_-(1-F_+)-K_+(1-F_-)=c(F_+-F_-) \tag{3.8}$$

which may be shown to hold[43] using Eqs. (3.2) and (3.7). This leads to the implicit equation

$$\psi=\frac{c_V-p_c(1-\chi)(1-\epsilon_+ g(\epsilon_+))}{1-p_c+p_c\epsilon_+ g(\epsilon_+)} - \frac{\chi p_c(1-\epsilon_- g(\epsilon_-))}{1-p_c+p_c\epsilon_- g(\epsilon_-)} \tag{3.9}$$

with

$$\epsilon_\pm=\frac{i\omega+\lambda_\pm}{\Gamma_0\psi}, \tag{3.9a}$$

and where

$$\chi=K_-\frac{1-F_+}{F_+-F_-}. \tag{3.9b}$$

Equations (3.9) constitute the most general final result of this paper and a departure point for numerical evaluation of ψ. We first examine a few special limits:

(a) For $\tau_A=\tau_B\equiv\tau$, namely, the A and B particles are identical, we have $\lambda_+=1/\tau$ and $\lambda_-=c_V/\tau$. We thus find $K_-=0$ and $F_+=1$ while $1-F_-$ is nonzero (see Appendix B). Therefore χ vanishes in this limit [like $(\tau_A-\tau_B)^2$]. Equation (3.9) reduces to

$$\psi=\frac{c_V-p_c+p_c\epsilon g(\epsilon)}{1-p_c+p_c\epsilon g(\epsilon)} \tag{3.10}$$

with

$$\epsilon=(i\omega+\tau^{-1})/(\Gamma_0\psi). \tag{3.10a}$$

This is the previously obtained result for the tracer effective hopping rate in a single component NILG.[16,37,38]

(b) For $\Gamma_0=\Gamma_B$ and $c_B\to 0$ we have a tracer B moving in an A background. This should again yield the single component result Eq. (3.10). Indeed, in this case we have from Eq. (3.2)

$$\lambda_\pm=\frac{1}{2}\left\{\frac{1-c_A}{\tau_B}+\frac{1}{\tau_A}\pm\left|\frac{1-c_A}{\tau_B}-\frac{1}{\tau_A}\right|\right\}. \tag{3.11}$$

If $(1-c_A)\tau_B^{-1}>\tau_A^{-1}$ we have $\lambda_+=(1-c_A)/\tau_B$ and $\lambda_-=1/\tau_A$. We therefore have $K_-=-c_A$ and $F_+\to\infty$ while F_- is finite. Thus $\chi=c_A$ and after some algebra we find that all the terms containing ϵ_+ vanish identically and Eq. (3.9) becomes identical to Eq. (3.10) with $c_V=1-c_A$, $\Gamma_O=\Gamma_B$ and $\tau=\tau_A$, as expected. For $(1-c_A)\tau_B^{-1}<\tau_A^{-1}$ we have $\lambda_+=1/\tau_A$ and $\lambda_-=(1-c_A)/\tau_B$, thus $F_-\to\infty$ while K_- and F_+ are finite. Hence $\chi\to 0$ and Eq. (3.10), with the same definitions for c_V, Γ_0, and τ, is again recovered.

(c) Consider the case where both $\Gamma_A/\Gamma_0\to 0$ and $\Gamma_B/\Gamma_0\to 0$, while their ratio Γ_A/Γ_B takes any finite value. In this case both A and B are infinitely slower then the tracer O and the latter undergoes a *single* particle diffusion in a static percolating network. Indeed, in this limit $\Gamma_0\tau_A^{-1}$, $\Gamma_0\tau_B^{-1}\to 0$ so $\lambda_\pm/\Gamma_0\to 0$ and we get again Eq. (3.10) now with $\epsilon=i\omega/(\Gamma_0\psi)$, which is the known EMA result for this case.[3-6] In particular, for $\omega=0$ we have $\psi=(c_V-p_c)/(1-p_c)$ for $c_V\geqslant p_c$ and 0 for $c_V\leqslant p_c$.

(d) In the opposite limit where $\Gamma_A/\Gamma_0\to\infty$ and $\Gamma_B/\Gamma_0\to\infty$ (but with arbitrary ratio Γ_A/Γ_B), or for $\omega/\Gamma_0\to\infty$, we have $\epsilon_\pm\to\infty$ as well and using[16] $\epsilon_\pm g(\epsilon_\pm)\to 1$ we get $\psi=c_V$—the mean-field result, which is the exact result for this limit.

The result (3.9) is parametrized by the density fluctuation times τ_A and τ_B which are expected to be dependent on the bare jump rates Γ_A and Γ_B and on the concentrations c_A and c_B. Next we consider this dependence in more detail.

IV. DENSITY FLUCTUATION TIMES

The fluctuation times τ_A and τ_B of Eq. (3.1) are typical parameters of dynamic percolation theory, however their determination in the context of the present application constitutes the main conceptual problem in this formalism. There is no unique rigorous way to obtain these parameters. For this reason, we propose a few possible options using plausible physical arguments, and contrast them with results of numerical simulations.

The simplest way, already described in Sec. II, is to use the mean-field jump rates of the A and B particles from a site which is NN to the tracer particle. These are $c_V(Z-1)\Gamma_A$ and $c_V(Z-1)\Gamma_B$ for the A and B particles respectively, where $Z-1$ instead of Z appears because the tracer site is excluded. Comparing these to the corresponding rates in Eq. (3.1), c_V/τ_A and c_V/τ_B, we find that [cf., Eq. (2.4)]

$$\tau_A^{-1}=(Z-1)\Gamma_A \tag{4.1a}$$

and

$$\tau_B^{-1}=(Z-1)\Gamma_B. \tag{4.1b}$$

This is a reasonable approximation in many situations. We note however that this choice disregards any possible dependence of τ_A and τ_B on the composition of the mixture. In particular, in the static A limit $\tau_A\to\infty$, one expects some effect of the percolation properties of the static random network made by the A particles on the fluctuation time τ_B. Such effects are absent in Eqs. (4.1).

With this in mind we shall follow our previous studies[16] and attempt to relate the fluctuations times to the chemical diffusion coefficients of the system. The rationale behind this approach is that the chemical diffusion rates are directly related to concentration fluctuations. In our binary mixture there are four such chemical diffusion coefficients: D_{AA}, D_{AB}, D_{BA}, and D_{BB}. They are defined as the coefficients of the two coupled phenomenological diffusion equations (see also Appendix C)

$$\frac{\partial}{\partial t}\begin{pmatrix}c_A(\mathbf{x},t)\\ c_B(\mathbf{x},t)\end{pmatrix}=\begin{pmatrix}D_{AA} & D_{AB}\\ D_{BA} & D_{BB}\end{pmatrix}\begin{pmatrix}\nabla^2 c_A(\mathbf{x},t)\\ \nabla^2 c_B(\mathbf{x},t)\end{pmatrix}. \tag{4.2}$$

Here the diffusion coefficients may depend in a complicated way on the concentrations $c_A=\langle c_A(\mathbf{x},t)\rangle$ and $c_B=\langle c_B(\mathbf{x},t)\rangle$, on the jump rates Γ_A and Γ_B, and on interaction parameters (in the interacting LG case). In this section we assume that these coefficients are known. In Sec. VII we give approximate practical expressions for these coefficients in the NILG case.

As a first step we write the discrete form of Eq. (4.2)

$$\frac{d}{dt}P_A(l,t) = D_{AA}\sum_{l'}[P_A(l',t) - P_A(l,t)] + D_{AB}\sum_{l'}[P_B(l',t) - P_B(l,t)], \quad (4.3a)$$

$$\frac{d}{dt}P_B(l,t) = D_{BA}\sum_{l'}[P_A(l',t) - P_A(l,t)] + D_{BB}\sum_{l'}[P_B(l',t) - P_B(l,t)], \quad (4.3b)$$

where $P_A(l,t)$ and $P_B(l,t)$ are the probabilities to find an A or B particle on site l at time t, respectively. Thus, the discretization is assumed to be valid on the same lattice on which the lattice gas was originally defined. We note however that a rigorous discretization of this type should probably lead to a non-Markovian equation.

Consider now Eq. (4.3) written for a site l which is NN to the tracer particle. The tracer site is then excluded from the sums over l' in the right hand side. To derive Eq. (3.1) we make a mean-field approximation by taking $P_A(l',t) = c_A$ and $P_B(l',t) = c_B$ for any $l' \neq l$. Then with $f(A,t) \equiv P_A(l,t)$ and $f(B,t) \equiv P_B(l,t)$ we have

$$\frac{d}{dt}f(A,t) = (Z-1)\{D_{AA}[c_A - f(A,t)] + D_{AB}[c_B - f(B,t)]\}, \quad (4.4a)$$

$$\frac{d}{dt}f(B,t) = (Z-1)\{D_{BA}[c_A - f(A,t)] + D_{BB}[c_B - f(B,t)]\}. \quad (4.4b)$$

On the other hand, using $f(V,t) = 1 - f(A,t) - f(B,t)$ in the first and third lines of Eq. (3.1) leads to

$$\frac{d}{dt}f(A,t) = -\frac{1-c_B}{\tau_A}f(A,t) - \frac{c_A}{\tau_A}f(B,t) + \frac{c_A}{\tau_A}, \quad (4.5a)$$

$$\frac{d}{dt}f(B,t) = -\frac{1-c_A}{\tau_B}f(B,t) - \frac{c_B}{\tau_B}f(A,t) + \frac{c_B}{\tau_B}. \quad (4.5b)$$

Comparing now Eqs. (4.5) to Eqs. (4.4) we find that they can be identical *only if*

$$\frac{D_{AB}}{D_{AA}} = \frac{c_A}{1-c_B}, \quad (4.6a)$$

$$\frac{D_{BA}}{D_{BB}} = \frac{c_B}{1-c_A}. \quad (4.6b)$$

If so, we have

$$\tau_A^{-1} = \frac{(Z-1)D_{AA}}{1-c_B}, \quad (4.7a)$$

$$\tau_B^{-1} = \frac{(Z-1)D_{BB}}{1-c_A}. \quad (4.7b)$$

However, conditions (4.6) do not generally hold, even in the NILG case considered here. If we use the linear relations given in Appendix C Eqs. (C12), between the Onsager coefficients Λ_{AA}, Λ_{BB}, and $\Lambda_{AB} = \Lambda_{BA}$ and the chemical diffusion coefficients defined above, we find that the relations (4.6) hold only if the cross Onsager coefficients vanish, namely, $\Lambda_{AB} = \Lambda_{BA} = 0$. On the other hand, both the simulation results of Kehr *et al.*[17] and some exact[26(a)] and approximate[24] results for limiting cases (see also Sec. VII) show that the cross Onsager coefficients may be of the order of the diagonal ones, so Eqs. (4.6) and (4.7) are not justified.

The validity of the mean-field dynamics used here, namely, of Eq. (3.1), is thus questionable.[44] Still, Eq. (3.1) seems intuitively to be a relatively good approximation to the single site occupation dynamics. Assuming that it holds, we limit ourselves to the question of determining the fluctuation times. If Eqs. (4.6) were correct then Eqs. (4.7) could have been written in other equivalent forms:

$$\tau_A^{-1} = \frac{(Z-1)D_{AB}}{c_A}, \quad (4.8a)$$

$$\tau_B^{-1} = \frac{(Z-1)D_{BA}}{c_B}, \quad (4.8b)$$

or

$$\tau_A^{-1} = (Z-1)\left(D_{AA} + \frac{c_B}{c_A}D_{AB}\right), \quad (4.9a)$$

$$\tau_B^{-1} = (Z-1)\left(D_{BB} + \frac{c_A}{c_B}D_{BA}\right). \quad (4.9b)$$

Since Eqs. (4.6) do not hold, we regard Eqs. (4.7)–(4.9) as distinct choices, with the best choice determined by other means.

A different approach, which does not rely on any assumption regarding the chemical diffusion coefficients, is as follows. Summing up Eqs. (4.4a) and (4.4b) leads to

$$\frac{d}{dt}f(A/B,t) = (Z-1)\{(D_{AA}+D_{BA})[c_A - f(A,t)] + (D_{AB}+D_{BB})[c_B - f(B,t)]\}, \quad (4.10)$$

where $f(A/B,t) = f(A,t) + f(B,t)$ is the probability to find a particle, either A or B, on site l. On the other hand, summing up lines 1 and 3 in Eq. (3.1) and using $f(V) = 1 - f(A) - (f(B)$, leads to

$$\frac{d}{dt}f(A/B,t) = -\left[\frac{1-c_B}{\tau_A} + \frac{c_B}{\tau_B}\right]f(A,t) - \left[\frac{1-c_A}{\tau_B} + \frac{c_A}{\tau_A}\right] \times f(B,t) + \frac{c_A}{\tau_A} + \frac{c_B}{\tau_B}. \quad (4.11)$$

Comparing now Eqs. (4.10) and (4.11) we find

$$\frac{1-c_B}{\tau_A} + \frac{c_B}{\tau_B} = (Z-1)(D_{AA}+D_{BA}), \quad (4.12a)$$

$$\frac{1-c_A}{\tau_B} + \frac{c_A}{\tau_A} = (Z-1)(D_{AB}+D_{BB}). \quad (4.12b)$$

Equations (4.12) lead to

$$\frac{1}{\tau_A}=\frac{Z-1}{c_V}\{(1-c_A)(D_{AA}+D_{BA}) - c_B(D_{AB}+D_{BB})\}, \tag{4.13a}$$

$$\frac{1}{\tau_B}=\frac{Z-1}{c_V}\{(1-c_B)(D_{BB}+D_{AB}) - c_A(D_{BA}+D_{AA})\}. \tag{4.13b}$$

Expressions (4.13) and (4.9) are identical. To show this we rewrite both equations in terms of the Onsager coefficients, using Eqs. (C12). Both Eqs. (4.9) and (4.13) then lead to

$$\frac{1}{\tau_A}=(Z-1)\frac{\Lambda_{AA}+\Lambda_{AB}}{c_A c_V}, \tag{4.14a}$$

$$\frac{1}{\tau_B}=(Z-1)\frac{\Lambda_{BB}+\Lambda_{AB}}{c_B c_V}. \tag{4.14b}$$

If we repeat the same procedure for Eqs. (4.7a) and (4.8a) we get, respectively,

$$\tau_A^{-1}=\frac{Z-1}{c_V}\left[\frac{\Lambda_{AA}}{c_A}+\frac{\Lambda_{AB}}{1-c_B}\right], \tag{4.15}$$

$$\tau_A^{-1}=\frac{Z-1}{c_A c_V}\left[\Lambda_{AA}+\Lambda_{AB}\frac{1-c_A}{c_B}\right] \tag{4.16}$$

(the expressions for τ_B are obtained by interchanging A and B). Note that the difference between these expressions appears only in the term containing Λ_{AB}.

Consider these different choices. The form of Eqs. (4.9) is intuitively appealing because it contains the contribution, for τ_A, for example, both from D_{AA} and D_{AB} with relative proportions determined by the concentrations. The fact that it is identical to Eq. (4.13), which was derived without any condition on the diffusion coefficients, supports its superiority. Above all, for the limiting case of identical A and B particles $\Gamma_A=\Gamma_B\equiv\Gamma$, we find, by using Eqs. (4.14) and exact relations between the Onsager coefficients [c.f., Eqs. (7.1)], that only this choice, besides the trivial choice Eqs. (4.1), yields exactly $\tau_A^{-1}=\tau_B^{-1}=(Z-1)\Gamma$ as required from consistency conditions [see discussion after Eq. (3.5)]. For these reasons we prefer this choice. (The other choices will be referred to for the sake of comparison.)

Consider finally the limit where one type of particles—say A— are static, namely, $\gamma=\Gamma_A/\Gamma_B\to 0$. In this case $\Lambda_{AB}/\Lambda_{BB}\to 0$ and all choices (discussed above), for the relation between the fluctuation time τ_B and the chemical diffusion coefficients, become identical [but different from Eq. (4.1b)]. On the other hand $\Lambda_{AB}\sim\Lambda_{AA}$ (see Sec. VII) and these choices for τ_A are different from each other. We discuss this limit in more detail in Sec. V.

V. CASE OF ONE STATIC COMPONENT

Here we consider the limit where (say) the A particles are much slower than the B particles, $\gamma=\Gamma_A/\Gamma_B\to 0$. Without considering any specific form for τ_A and τ_B, we clearly have in this limit $\tau_A/\tau_B\to\infty$ (all the choices given in Sec. IV yield this result). Hence we find [from Eq. (3.2)]

$$\lambda_+=\frac{1-c_A}{\tau_B} \tag{5.1a}$$

and

$$\lambda_-\simeq\frac{c_V}{1-c_A}\tau_A^{-1}. \tag{5.1b}$$

This, with Eqs. (3.9b) and (3.7), then lead to

$$\chi=\frac{c_A c_V}{1-c_A}. \tag{5.2}$$

Focusing our attention on the tracer particle we consider two situations: $\Gamma_0\sim\Gamma_B$ and $\Gamma_0\sim\Gamma_A$. Consider first the case of a fast moving tracer $\Gamma_0\sim\Gamma_B$ (i.e., $\Gamma_A/\Gamma_0\to 0$). In the absence of B particles this situation corresponds to diffusion of the tracer particle in a static random network where the randomness is caused by the static distribution of A particles. In the presence of B particles ($c_B\neq 0$) and if $\Gamma_0=\Gamma_B$ this calculation yields the tracer diffusion coefficient of (identical) particles with hard core interaction diffusing in a random lattice. From Eqs. (5.1) $\lambda_-/\Gamma_0\to 0$ while λ_+/Γ_0 is finite. Thus in Eq. (3.9) we have $\epsilon_-=i\omega/(\Gamma_0\psi)$. In particular, for the DC limit ($\omega=0$) we have $\epsilon_-=0$ and

$$\psi=\frac{c_V-p_c(1-\chi)(1-\epsilon_+ g(\epsilon_+))}{1-p_c+p_c\epsilon_+ g(\epsilon_+)}-\frac{\chi p_c}{1-p_c}, \tag{5.3}$$

$$\epsilon_+=\frac{(1-c_A)\tau_B^{-1}}{\Gamma_0\psi}. \tag{5.3a}$$

For concentrations $c_B\leqslant p_c$, this equation exhibits a threshold at $c_A=1-p_c$ for any choice of nonzero $(\Gamma_0\tau_B)^{-1}$. This may be seen by putting $\psi=0$ on both sides of Eq. (5.3). (In this way one also finds the obvious result that $\psi=0$ when $c=c_A+c_B=1$.) Thus, the tracer percolation threshold *does not depend* on the concentration of the moving B particles, as can be expected intuitively.

In Eq. (5.3) we consider two possibilities. First,

$$\tau_B^{-1}=(Z-1)\Gamma_B \tag{5.4a}$$

which is the mean-field approximation, Eq. (4.1b). Second,

$$\tau_B^{-1}=(Z-1)\frac{\Lambda_{BB}}{c_B c_V}=(Z-1)\frac{D_{BB}}{1-c_A}, \tag{5.4b}$$

which is obtained from Eqs. (4.14)–(4.16) (all are identical in this limit) and (C12d), using the fact that $\Lambda_{AA}/\Gamma_B\to 0$ and $\Lambda_{AB}/\Gamma_B\to 0$ as $\gamma\to 0$. D_{BB} in this case does not depend on the concentration of B particles and is identical to the single particle diffusion coefficient on the same disordered lattice [see Refs. 14(a), 14(c), 19, and 22 and Appendix D]. If we use for it the EMA result, $D_{BB}=(1-c_A-p_c)/(1-p_c)$ for $1-c_A>p_c$, we get

$$\tau_B^{-1}=\Gamma_B(Z-1)\frac{1-c_A-p_c}{(1-c_A)(1-p_c)}. \tag{5.5}$$

According to Eqs. (5.4b) or (5.5) τ_B^{-1} vanishes at the percolation threshold created by the static A particles (i.e., when $c_A=1-p_c$) because D_{BB} vanishes at that concentration. There is however an important difference between D_{BB}

and τ_B: the former is a global transport coefficient which is effected by relatively long range features of the network while the latter is a (disorder averaged) local property which should not necessarily vanish at the percolation threshold. In fact, the exact *disorder averaged* occupation dynamics of the B particles (and the resulting mean-field local rate equation), written on the same lattice on which the LG is defined, is a non-Markovian equation [cf., Eq. (2.6)], in contradiction to the assumption made in Eq. (3.1). This non-Markovian equation becomes Markovian only in the short time and the long time limits leading to Eqs. (5.4a) and (5.4b), respectively. A possible way to improve the Markovian approximation is to recognize that we are interested in the density fluctuations of the B particles (and in the corresponding τ_B) only on a timescale Γ_0^{-1} for the jump of the tracer particle. A possibly better ansatz is therefore to use in Eq. (5.4b) the frequency-dependent diffusion coefficient $D_{BB}(\omega)$ at finite ω, where $\omega \sim \Gamma_0$ ($\sim \Gamma_B$) is the most likely choice. This means that τ_B must be bounded by its $\omega = 0$ and $\omega \to \infty$ limits, namely,

$$\Gamma_B(Z-1)\frac{1-c_A-p_c}{(1-c_A)(1-p_c)} \leqslant \tau_B^{-1} \leqslant \Gamma_B(Z-1). \tag{5.6}$$

It is found (see Sec. VIII) that the result for the tracer diffusion coefficient is only weakly sensitive to the choice of τ_B in this range for concentration far enough from the threshold. Very close to the percolation threshold the sensitivity to τ_B is large. To analyze the behavior of ψ near the threshold we use,[16] for $\epsilon \to \infty$ ($\psi \to 0$; this holds also for $c_V \to 0$) $g(\epsilon) \simeq \epsilon^{-1} - Z\epsilon^{-2}$. This leads to

$$\psi \simeq \frac{c_V(1-c_A)(1-c_A-p_c)}{(1-p_c)[(1-c_A)^2 + 2c_B\tau_B\Gamma_0]}. \tag{5.7}$$

Using the upper bound for τ_B^{-1} Eq. (5.4a) in Eq. (5.7) (with $1-c_A \simeq p_c$) then leads to

$$\psi \simeq \frac{c_V(Z-1)p_c}{(1-p_c)[(Z-1)p_c^2 + 2c_B\Gamma_0/\Gamma_B]}(1-c_A-p_c). \tag{5.7a}$$

Thus, ψ is linear in $1-c_A-p_c$. The proportionality factor is smaller then in the single particle case ($c_B = 0$), where it is $(1-p_c)^{-1}$. On the other hand, the critical exponent $\nu = 1$ in $\psi \sim (1-c_A-p_c)^{\nu}$ is the same as in the single particle case, which may be expected when τ_B^{-1} in Eq. (5.7) has a finite value at the threshold. This is consistent with the numerical simulations of Harder *et al.*[23] for a specific 2-*d* correlated site percolation model, and also with the simulation results of Heupel[20] for a 3-*d* random site percolation model. In the latter simulation the exponent k of the anomalous diffusion behavior at the percolation threshold—$\langle r^2(t)\rangle \sim t^k$—was found to be identical with the corresponding single particle exponent. Together with a scaling assumption of the type given in Refs. 1 or 7, this means that the critical exponent for the diffusion coefficient is also the same.[19]

On the other hand, using the (EMA) lower bound Eq. (5.5) in Eq. (5.7) yields (for $1-c_A-p_c \ll c_B$)

$$\psi \simeq \frac{\Gamma_B}{\Gamma_0}\frac{(Z-1)c_V}{2(1-p_c)^2c_B}(1-c_A-p_c)^2. \tag{5.8}$$

Thus, the critical exponent ν is changed (i.e., $\nu = 2$). As $c_B \to 0$, the region where Eq. (5.8) remains valid ($1-c_A-p_c \ll c_B$) gets smaller and we have a crossover to the single particle EMA critical behavior with critical exponent $\nu = 1$. As noted, this behavior is not observed in numerical simulations.

We now turn to the case of $\Gamma_0 \sim \Gamma_A$ (i.e., $\Gamma_0/\Gamma_B \to 0$). Thus, from Eq. (5.1) one has $\lambda_+/\Gamma_0 \to \infty$ while λ_-/Γ_0 is finite. Using then $\epsilon_+ g(\epsilon_+) \to 1$ for $\epsilon_+ \to \infty$ in Eq. (3.9), we have

$$\psi = c_V\left\{1 - \frac{c_Ap_c}{1-c_A}\left[\frac{1-\epsilon_- g(\epsilon_-)}{1-p_c+p_c\epsilon_- g(\epsilon_-)}\right]\right\} \tag{5.9}$$

and

$$\epsilon_- = \left(i\omega + \frac{c_V}{(1-c_A)\tau_A}\right)\Big/\Gamma_0\psi. \tag{5.9a}$$

If $\Gamma_0 = \Gamma_A$ this yields the tracer diffusion coefficient of the A particles in the presence of the fast moving B background. Note that the presence of the B particles enters in this limit only through c_V. Also note that for finite frequencies $-\psi < c_V$, i.e., the correlation factor f defined by $\psi = c_Vf$ is *smaller* then 1 (except for the limiting case $c_A \to 0$).

VI. THE SMALL VACANCY CONCENTRATION LIMIT

The small vacancy concentration limit $c_V \to 0$ is of particular importance because of its applicability to disordered binary alloys and we therefore analyze it separately. For $c_V \to 0$ Eq. (3.2) yields

$$\lambda_+ = \frac{c_B}{\tau_B} + \frac{c_A}{\tau_A}, \tag{6.1a}$$

$$\lambda_- \simeq \frac{c_V}{c_B\tau_A + c_A\tau_B}, \tag{6.1b}$$

where $c_A + c_B = 1$. Thus $\lambda_- \to 0$ while λ_+ remains finite at this limit. Eqs. (3.7) and (6.1) then lead to

$$K_- = \frac{c_Vc_A(\tau_B - \tau_A)}{c_A\tau_B + c_B\tau_A}, \tag{6.2a}$$

$$F_+ = \frac{\tau_A}{\tau_B}, \tag{6.2b}$$

$$F_- = -\frac{c_A}{c_B}, \tag{6.2c}$$

and χ of Eq. (3.9b) becomes

$$\chi = \frac{c_Vc_Ac_B(\tau_B - \tau_A)^2}{(c_A\tau_B + c_B\tau_A)^2}. \tag{6.3}$$

For $c_V \to 0$, ψ and λ_- are $o(c_V)$ so for $\omega = 0$ we have $\epsilon_+ \to \infty$ while ϵ_- remains finite. Using, for $\epsilon \to \infty$, $g(\epsilon) \simeq \epsilon^{-1} - Z\epsilon^{-2}$ we find from Eq. (3.9) that the correlation factor $f \equiv f(c \to 1)$ of the tracer O, defined as $\psi = c_Vf(c)$,

is a solution of

$$f=\left\{1-p_c c_A c_B\left[\frac{(\tau_B-\tau_A)^2}{(c_A\tau_B+c_B\tau_A)^2}\right]\times\left[\frac{1-\epsilon_- g(\epsilon_-)}{1-p_c+p_c\epsilon_- g(\epsilon_-)}\right]\right\}\Big/\left(1+\frac{2\Gamma_0}{c_A\tau_A^{-1}+c_B\tau_B^{-1}}\right), \tag{6.4}$$

where

$$\epsilon_- = [\Gamma_0(c_A\tau_B+c_B\tau_A)f]^{-1}. \tag{6.4a}$$

In the single component limit, either $c_A\to 0$ ($c_B\to 1$) whereas $\tau_B^{-1}=(Z-1)\Gamma_B$ [cf. Eqs. (4.1) and (4.14)], or $c_B\to 0$ and $\tau_A^{-1}=(Z-1)\Gamma_A$, or $\Gamma_A=\Gamma_B\equiv\Gamma[(\tau_A^{-1}=\tau_B^{-1})=(Z-1)\Gamma]$. In this case Eq. (6.4) reduces to $f=(Z-1)/(Z-1+2\gamma')$, where $\gamma'=\Gamma_0/\Gamma$ with Γ being the jump rate of the background particles. This is our previous result for the correlation factor in the one component system.[16]

Consider now again the limit $\gamma=\Gamma_A/\Gamma_B\to 0$. If the tracer is a B particle we get again the result implied by Eq. (5.7) (with $\Gamma_0=\Gamma_B$ and $c_B=1-c_A$)

$$f_B=\frac{(1-c_A-p_c)}{(1-p_c)[1-c_A+2\tau_B\Gamma_B]}. \tag{6.5}$$

The critical behavior of this equation was already discussed in Sec. V. Note again that for the single component case $c_A\to 0$, we get for the self-diffusion correlation factor $f_B=(Z-1)/(Z+1)$, our previous result.[16] If the tracer is an A particle, $\Gamma_0=\Gamma_A$ and Eq. (6.4) [or Eq. (5.7)] leads to

$$f_A=1-p_c\frac{1-c_B}{c_B}\left[\frac{1-\epsilon_- g(\epsilon_-)}{1-p_c+p_c\epsilon_- g(\epsilon_-)}\right] \tag{6.6}$$

with

$$\epsilon_- = (c_B\Gamma_A\tau_A f_A)^{-1}. \tag{6.6a}$$

Taking the single component limit $c_B\to 0$, using $g(\epsilon_-)\simeq\epsilon_-^{-1}-Z\epsilon_-^{-2}$, leads again to $f_A=(Z-1)/(Z+1)$. For $c_B\to 1$ ($c_A\to 0$) w get $f_A=1$, as expected for a single particle in an infinitely fast moving background. However, for $c_B<1$ ($c_A>0$) we get $f_A<1$.

The latter result is in contradiction with that obtained by Sato and Kikuchi[25] by a reformulation of the path probability method. According to them, for all $c_B\geqslant p_c$ in the limit under consideration ($c_V\to 0,\gamma\to 0$) one has $f_A=1$. Appealing argument for this result[45] is the fact that in this range of concentrations there exists an infinite B cluster, thus enabling the vacancy to move infinitely fast (relative to the A motion) through the whole system, and therefore, after the A tracer has made a jump, the vacancy may appear with equal probability at any side of it. However, this argument ignores the motion of the A particles in A type clusters, which is clearly controlled by backward correlations. This counter argument is particularly strong if $p_c<\frac{1}{2}$. Then, in the range of concentrations $p_c<c_B<1-p_c$, there is an infinite cluster of A particles (coexistent with an infinite B cluster) and the A motion in this cluster may contribute substantially to the tracer diffusion coefficient. We note that our result[16] for the single component LG and in this $c\to 1$ limit is identical to the result of a former version of the path probability method due to Kikuchi.[10] This old version, however, does not lead to a percolation threshold for a binary mixture in the static limit.[25]

VII. CHEMICAL DIFFUSION COEFFICIENTS

In Sec. IV we have used the four chemical diffusion coefficients of the binary mixture, D_{AA}, D_{AB}, D_{BA}, and D_{BB}, to find the fluctuation times τ_A and τ_B (needed for the calculation of the tracer diffusion constant), assuming these coefficients to be known. In this section we obtain approximate expressions for these coefficients that will be used in the calculation of the tracer diffusion coefficient using the expressions of Sec. III. Other theories appear in the literature,[26(b),27] but those seem to break down for either small or large jump rate ratios.

First consider some exact relations. In a general interacting LG, only three of these diffusion coefficients are independent, because of the symmetry in the Onsager coefficients $\Lambda_{AB}=\Lambda_{BA}$ and the generalized Einstein relations [cf., Eqs. (C12)]. For the NILG case, Moleko and Allnatt[26(a)] have obtained two other exact relations

$$\frac{\Lambda_{AA}}{\Gamma_A}+\frac{\Lambda_{AB}}{\Gamma_B}=c_A c_V, \tag{7.1a}$$

$$\frac{\Lambda_{AB}}{\Gamma_A}+\frac{\Lambda_{BB}}{\Gamma_B}=c_B c_V. \tag{7.1b}$$

With these relations, there is only one independent Onsager coefficient. These relations may serve to find limiting expressions. Eliminating Λ_{AB} from Eqs. (7.1) we get

$$\Lambda_{AA}=\Gamma_A c_A c_V+\gamma^2\Lambda_{BB}-\gamma\Gamma_A c_B c_V, \tag{7.2}$$

where $\gamma=\Gamma_A/\Gamma_B$. When $\gamma\to 0$ we have $\Lambda_{AA}\to\Gamma_A c_A c_V$. To the first order in γ

$$\Lambda_{AA}\simeq\Gamma_A c_V(c_A-\gamma\delta),\quad \gamma\to 0, \tag{7.3}$$

where δ is independent of γ. Thus from Eq. (7.2) we have

$$\Lambda_{BB}=\Gamma_B c_V(c_B-\delta),\quad \gamma\to 0. \tag{7.4}$$

This means that δ is a function of the concentrations such that $\delta=c_B$ for $c_A=1-p_c$, the percolation threshold. We will get back to the calculation of δ later. Using Eq. (7.3) in Eq. (7.1a) we also find for this limit

$$\Lambda_{AB}=\Gamma_A c_V\delta,\quad \gamma\to 0 \tag{7.5}$$

which means that Λ_{AB} is of the same order of magnitude as Λ_{AA} (or smaller), the diagonal Onsager coefficient of the slow component. Thus $\Lambda_{AB}/\Lambda_{BB}\to 0$ for this limit and, from Eq. (C12d), we then have

$$D_{BB}=\Lambda_{BB}\frac{1-c_A}{c_B c_V},\quad \gamma\to 0. \tag{7.6}$$

As mentioned before, in this limit D_{BB} is identical to the diffusion coefficient of a single B particle on the same disordered lattice. Using the EMA expressions for the latter, namely, $D_{BB}=(1-c_A-p_c)/(1-p_c)$ for $c_A\geqslant 1-p_c$ and $D_{BB}=0$ for $c_A\leqslant p_c$, and using also Eqs. (7.4) and (7.6)

we obtain the following EMA result for δ

$$\delta=\begin{cases}\dfrac{p_c}{1-p_c}\dfrac{c_B c_A}{1-c_A} & c_A\leqslant 1-p_c\\ c_B & c_A\geqslant 1-p_c\end{cases}. \tag{7.7}$$

Together with Eq. (C12a) this leads to the following limiting result (to zero order in γ)

$$D_{AA}=\begin{cases}\Gamma_A\left[1-\dfrac{c_B(1-c_A-p_c)}{(1-c_A)(1-p_c)}\right] & c_A\leqslant 1-p_c\\ \Gamma_A & c_A\geqslant 1-p_c\end{cases},$$
$$\gamma\to 0. \tag{7.8}$$

The result (7.8) has the surprising feature that for $c_A\geqslant 1-p_c$, namely, when there is no infinite cluster of sites that are unoccupied by A particles, $D_{AA}=\Gamma_A$ which is identical to the result obtained for $c_B=0$ (one component system). Another interesting point is that when c_A increases from zero, D_{AA} becomes *larger* than the mean-field value, $D_{AA}\geqslant\Gamma_A(1-c_B)$ where the equal sign holds in the limit. Indeed, equality is expected for a single A particle in an infinitely fast B background.

For finite jump rate ratio γ we again need to calculate at least one (either chemical diffusion or Onsager) coefficient. Let us start with the observation that for a one component NILG with time-dependent bond disorder, where the bonds fluctuate *independently* of the LG motion, the chemical diffusion coefficient is identical to the single particle diffusion coefficient on the same dynamically disordered lattice (see Appendix D). This generalizes the known similar results[14(a),14(c),19,22] for static disorder or for ordered lattices. For a binary mixture LG we can regard one component—say B—as the LG and the dynamical bond disorder as due to the motion of the A. An approximate solution can be obtained if we assume in addition that the motion of A is independent of the B particles (but not vice versa). This is expected to be valid for small γ or small c_B. In this case we have again the situation discussed in Appendix D (this is of course a very rough approximation). Using the result obtained previously[16] for a single particle in a dynamically disordered lattice we get for $\omega=0$ (in the EMA)

$$D_{BB}=\Gamma_B\left[1-\frac{c_A}{1-p_c+p_c\epsilon_A g(\epsilon_A)}\right] \tag{7.9}$$

with

$$\epsilon_A=\frac{(Z-1)D_{AA}}{D_{BB}}. \tag{7.9a}$$

To find D_{BB} explicitly the following exact relation between D_{AA} and D_{BB} [obtained from Eqs. (7.1) and (C12)]

$$[D_{AA}-\Gamma_A(1-c_B)]\left[1-\frac{1-c_A}{\gamma c_B}\right]$$
$$=[D_{BB}-\Gamma_B(1-c_A)]\left[1-\frac{\gamma(1-c_B)}{c_A}\right] \tag{7.10}$$

can be used.

The result (7.9) should hold for small γ. Indeed, for $\gamma\to 0$ Eq. (7.9) yields the EMA result for the motion of B in a static random lattice. For $\gamma\to\infty$ however Eq. (7.9) yields $D_{BB}=\Gamma_B(1-c_A)$ in contradiction with the result obtained from Eq. (7.8) by interchanging A and B. An expression valid for large γ may be obtained however by interchanging A and B in Eq. (7.9).

For $c_B\to 0$ we have (for any γ) $D_{AA}\to\Gamma_A$ and Eq. (7.9) yields the EMA result for D_{tB}, the tracer diffusion coefficient of a single B in a background of A particles, obtained in our previous work[16] (namely, $D_{BB}=D_{tB}$ as should be in this limit). Using this expression in Eq. (7.10) we can solve for D_{AA} corrected to low order in c_B. Note that Eq. (7.10) provides an exact value for D_{AA} (and D_{BB}) at a specific intermediate point: For $\gamma(1-c_B)=c_A$ the right hand side of Eq. (7.10) vanishes and we get $D_{AA}=\Gamma_A(1-c_B)$. Similarly, for $\gamma c_B=1-c_A$ we have $D_{BB}=\Gamma_B(1-c_A)$.

To test Eq. (7.9) for $\gamma\ll 1$ we have solved numerically this equation together with Eq. (7.10) for $\gamma=0.1$. In Table I we compare these results for D_{AA} and D_{BB} to the results obtained from numerical simulations.[17] The agreement is better than 4% for all values. This suggests that in practice we may use Eqs. (7.9) and (7.10) at least for $\gamma\leqslant 0.1$ in order to obtain the chemical diffusion coefficients needed for the calculation of the tracer diffusion coefficient.

To end this section we rewrite the resulting fluctuation times τ_A and τ_B of Eqs. (4.14) in terms of D_{BB} and D_{AA}. Using Eqs. (7.1) and (C12), Eqs. (4.14) may be written as

$$\frac{1}{\tau_A}=(Z-1)\frac{\Gamma_A c_V+(\gamma-1)D_{AA}}{\gamma(1-c_B)-c_A}, \tag{7.11a}$$

$$\frac{1}{\tau_B}=(Z-1)\frac{\Gamma_B c_V+(\gamma^{-1}-1)D_{BB}}{\gamma^{-1}(1-c_A)-c_B}. \tag{7.11b}$$

In the limit $\gamma\to 0$ and within the EMA Eq. (7.11a) leads to

$$\frac{1}{\tau_A}=\begin{cases}(Z-1)\Gamma_A\left[1+\dfrac{p_c}{1-p_c}\dfrac{c_B}{1-c_A}\right] & c_A\leqslant 1-p_c\\ (Z-1)\Gamma_A\left(1+\dfrac{c_B}{c_A}\right) & c_A\geqslant 1-p_c\end{cases} \tag{7.12}$$

while τ_B [Eq. (7.11b)] reduces to Eq. (5.5). Note that since the slope of τ_A as a function of c_A is discontinuous at $c_A=1-p_c$, the resulting tracer diffusion coefficient of the

TABLE I. Theoretical and simulation results for the chemical diffusion coefficients D_{AA} and D_{BB} in a simple cubic lattice for $\gamma=\Gamma_A/\Gamma_B=0.1$.

c_V	c_A/c_B	D_{AA} [a]	D_{AA} [b]	D_{AA} [c]	D_{BB} [a]	D_{BB} [b]	D_{BB} [c]
0.01	1.0	0.0686	0.0673	0.0663	0.319	0.333	0.321
0.04	0.5	0.0489	0.0478	0.0472	0.540	0.552	0.534
0.04	1.0	0.0686	0.0673	0.0669	0.337	0.351	0.337
0.04	2.0	0.0843	0.0834	0.0819	0.173	0.183	0.176
0.10	1.0	0.0687	0.0676	0.0681	0.375	0.388	0.378

[a] From Eqs. (7.9) and (7.10) using the EMA p_c, $p_c=0.3333$.
[b] From Eqs. (7.9) and (7.10) using the exact p_c, $p_c=0.3117$.
[c] Simulation results from Ref. 17. Obtained using simulation data for the Onsager coefficients and Eqs. (C12).

A particles also exhibits a change in its slope at this point [cf., Eq. (6.6)].

VIII. NUMERICAL RESULTS AND DISCUSSION

In this section we present some numerical results based on our general result Eq. (3.9) and on the result for the static A limit ($\gamma \to 0$), Eq. (5.3) (which corresponds to particles B with interparticle hard core interactions moving on a random lattice created by the distribution of A particles), and compare them to numerical simulations. For the density fluctuation times we use Eq. (7.11), (7.12), and (5.5), henceforth referred to as choice (i). We also use, for sake of comparison, the mean-field expressions Eqs. (4.1) [choice (ii)]. The expressions used for the lattice Green's function of the origin $g(\epsilon)$ for the square, simple cubic, and face-centered-cubic lattices are summarized in Appendix E.

Our simulations were performed on a 100×100 square lattice with periodic boundary conditions using standard Monte Carlo technique. Three runs were performed for each composition, for different realizations of the (randomly chosen) lattice. The simulations were carried up to 100 000 Monte Carlo steps per particle, determined separately for each composition. The tracer diffusion coefficient was obtained from

$$D = \lim_{t \to \infty} \frac{\langle (\mathbf{r}(t) - \mathbf{r}(0))^2 \rangle}{4t} \tag{8.1}$$

(t is the time) where the average was performed over all diffusing particles (of the same kind). The error obtained is within 5% for most cases except for the static A case near the percolation threshold ($1 - c_A - p_c \sim 0.02$) where the simulation times were too short.

In Figs. 1–3 we present some numerical solutions of Eq. (5.3) with $\Gamma_0 = \Gamma_B$ for the tracer diffusion coefficient of the fast particles (B) in the *static* A limit, on square (Figs. 1–2) and simple cubic (Fig. 3) lattices, and compare them to results of numerical simulations.

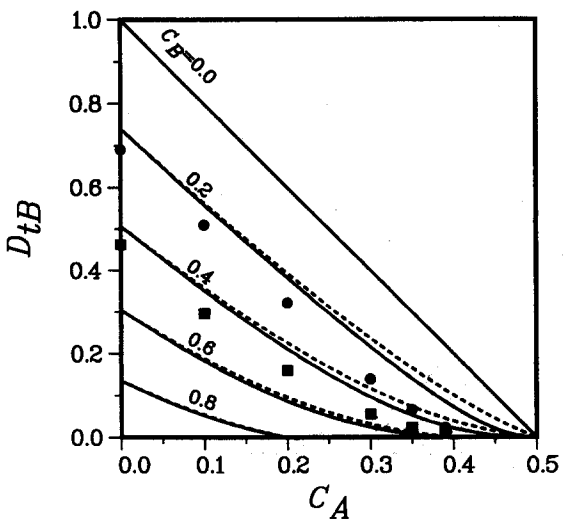

FIG. 1. Tracer diffusion coefficient D_{tB} in a static A background on a square lattice, plotted against c_A for different concentrations c_B ($\omega = 0$). The results are solutions to Eq. (5.3) using Eqs. (5.5) (full lines) and (5.4a) (dashed lines) for τ_B. The EMA percolation threshold $p_c = 0.5$ was used in both cases. The symbols represent our simulation results for $c_B = 0.2$ (circles) and $c_B = 0.4$ (squares). The estimated error of these results is within 5% for $c_A < 0.35$ and about 25% for $c_A = 0.39$.

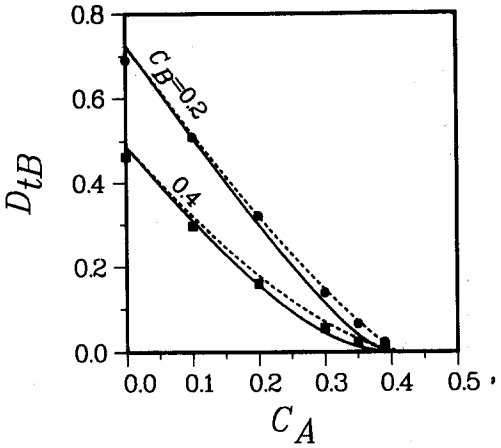

FIG. 2. The lines are the same as in Fig. 1 but with the use of $p_c = 0.592\,75$ instead of 0.5. The symbols are the same simulation results shown in Fig. 1.

Figure 1 shows the tracer diffusion coefficient D_{tB} (in units of $\Gamma_B a^2$ where a is the lattice constant) of a tracer B particle, in a static A background and on a square lattice, as a function of c_A and for different concentrations c_B. The full lines result from using choice (i) for τ_B while the dashed lines are based on choice (ii). It is seen that the mean-field approximation for τ_B is already quite adequate for small c_A; the differences between the two choices is largest for intermediate c_A values close to p_c and both become identical for $c_A = 0$ and, of course for $1 - c_A = p_c$, where $D_{tB} = 0$. Close to p_c it can be seen that for choice (ii) $D_{tB} \sim (1 - c_A - p_c)^2$ as implied by Eq. (5.8) while for choice (i) $D_{tB} \sim 1 - c_A - p_c$. It should be noted that by the nature of our approximation, the percolation threshold at this static A limit is obtained at $1 - c_A = p_c = 2/Z$ ($= 0.5$ for a square lattice), corresponding to a bond percolation model. However, the actual situation is that of a static distribution of A

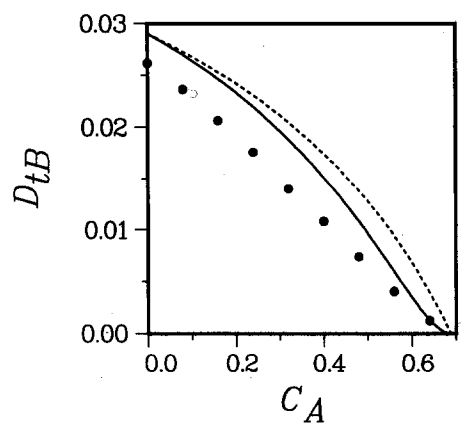

FIG. 3. Tracer diffusion coefficient D_{tB} in a simple cubic lattice with a static A background for a constant $c_V = 1 - c_A - c_B = 0.039\,16$ ($\omega = 0$). The lines are based on solutions to Eq. (5.3) using Eqs. (5.5) (full line) and (5.4a) (dashed line) for τ_B. The exact value for the threshold $p_c = 0.311\,7$ (instead of the EMA result 0.333) has been used. The symbols are simulation results of Braun and Kehr (Ref. 19) and have an error less than 2%.

particles blocking random network sites, and is therefore a site percolation problem where the actual percolation threshold (for a square lattice) is[1] $p_c = 0.592\,75$. Thus, our calculation for this site percolation problem contains an inherent error which is mainly manifested at the p_c region. We have previously shown[16] that a substantial improvement of the results may be obtained by replacing p_c in expressions like (3.9) or (5.3) by the *actual* percolation threshold of the lattice under consideration. This is shown in Fig. 2 where the calculation based on Eq. (5.3) and choices (i) (full line) or (ii) (dashed line) is repeated using $p_c = 0.592\,75$. We see that both choices for τ_B lead to a good agreement with the simulation results. In fact, within the accuracy of our simulations both choices work equally well.[46]

Similar results for a simple cubic lattice are shown in Fig. 3. Here we use a constant value for c_V, $c_V = 0.039\,16$. This is not quite the small vacancy concentration limit and we use Eq. (5.3) rather than the limiting result Eq. (6.5). Again we use the exact value for the site percolation threshold[1] $p_c = 0.311\,7$ instead of the EMA result $p_c = \frac{1}{3}$. The results are compared to the simulation results of Braun and Kehr.[19] Here the difference between the two choices for τ_B is clearly seen even not very close to the threshold. Note again that the critical exponent 2 [c.f., Eq. (5.8)] is indeed seen for the solid line [choice (i)] near the threshold. The EMA results again overestimate the exact diffusion rate because of the other approximations (neglect of correlations) involved.

In Fig. 4 we present the EMA and numerical simulation results for the tracer correlation factor f_B ($= D_{tB}/c_V$) in a 2 dimensional square lattice, for $\gamma = \Gamma_A/\Gamma_B = 100$, 0.01 using a constant and small c_V value, $c_V = 0.04$. The simulation results shown here are from Kehr *et al.*[17] The EMA results are from Eq. (3.9) [the limiting equation (5.9) is not completely reached] using $\omega = 0$ and $p_c = 0.592\,75$. For each γ value we have used both choices (i) and (ii) for τ_A and τ_B. The results for both γ value are in a reasonable agreement with the simulation results; the reasons for the small discrepancies were discussed above. The results obtained using choice (i) for $\gamma = 100$ (solid line) show a change in the slope near $c_B = p_c$, whereas the mean-field choice (ii) (dashed line) does not show such an effect. The simulation results seem to disagree with choice (i) and especially with the theoretical results of Sato and Kikuchi[25] where the change in the slope is much more pronounced (see discussion at the end of Sec. VI). We note however that since only three simulation data are presented with only one for $c_B > p_c$ ($c_B = 0.64$) and since both static and small vacancy concentration limits are not completely reached, no final conclusion can be made.

Results for larger rate of A motion are shown in Figs. 5(a) and 5(b). Here we show, for $\gamma = 0.1$, D_{tB} (in units of $\Gamma_B a^2$) as a function of c_A for several values of c_B, for a 2 dimensional square lattice, using $p_c = 0.5$ [Fig. 5(a)] and $p_c = 0.592\,75$ [Fig. 5(b)]. Our simulation results for $c_B = 0.1$, 0.2, and 0.3 are in very good agreement with the theory provided that the latter value of p_c is used [Fig. 5(b)]. In both figures we have used only choice (i) for τ_A and τ_B. However, for this and larger values of γ the two choices for τ_A and τ_B yield almost identical results, differing by less than 1%. It is interesting to note the crossover from

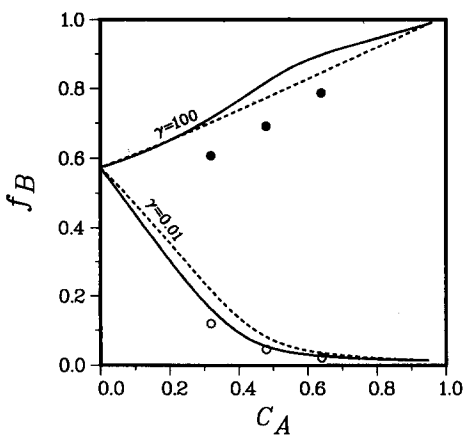

FIG. 4. Tracer correlation factor f_B ($= D_{tB}/c_V$) in a square lattice, for $\gamma = \Gamma_A/\Gamma_B = 100$ and $\gamma = 0.01$, and for a constant $c_V = 0.04$ ($\omega = 0$). The lines are solutions to Eq. (3.9) using $\omega = 0$, the exact threshold value $p_c = 0.592\,75$, and Eqs. (7.11) (full lines) and (4.1) (dashed lines) for τ_A and τ_B. The symbols are simulation results of Kehr *et al.* (Ref. 17).

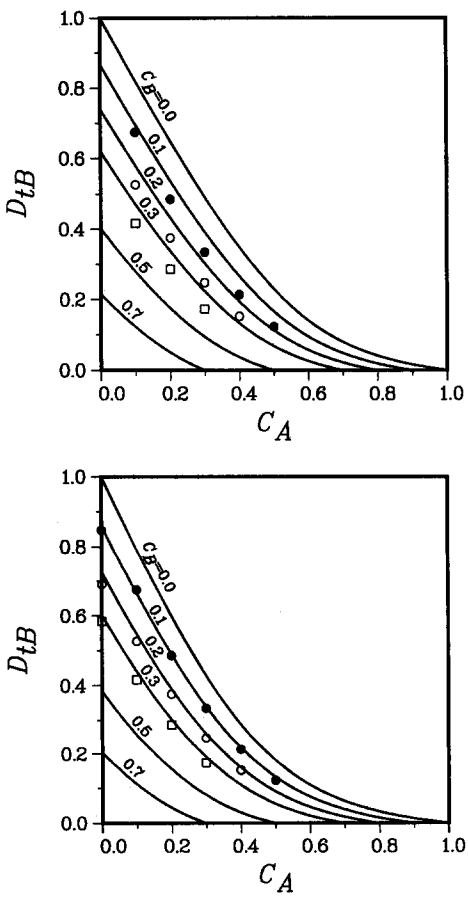

FIG. 5. Tracer diffusion coefficient D_{tB} for $\gamma = \Gamma_A/\Gamma_B = 0.1$ in a square lattice ($\omega = 0$). The lines are solutions to Eq. (3.9), using the EMA threshold $p_c = 0.5$ [Fig. 5(a)] and the exact threshold $p_c = 0.592\,75$ [Fig. 5(b)]. Equations (7.11) were used for τ_A and τ_B. The results of using Eqs. (4.1) for these times are less than 1% different from those plotted. The symbols are our simulation results: filled circles—$c_B = 0.1$, open circles—$c_B = 0.2$, open squares—$c_B = 0.3$.

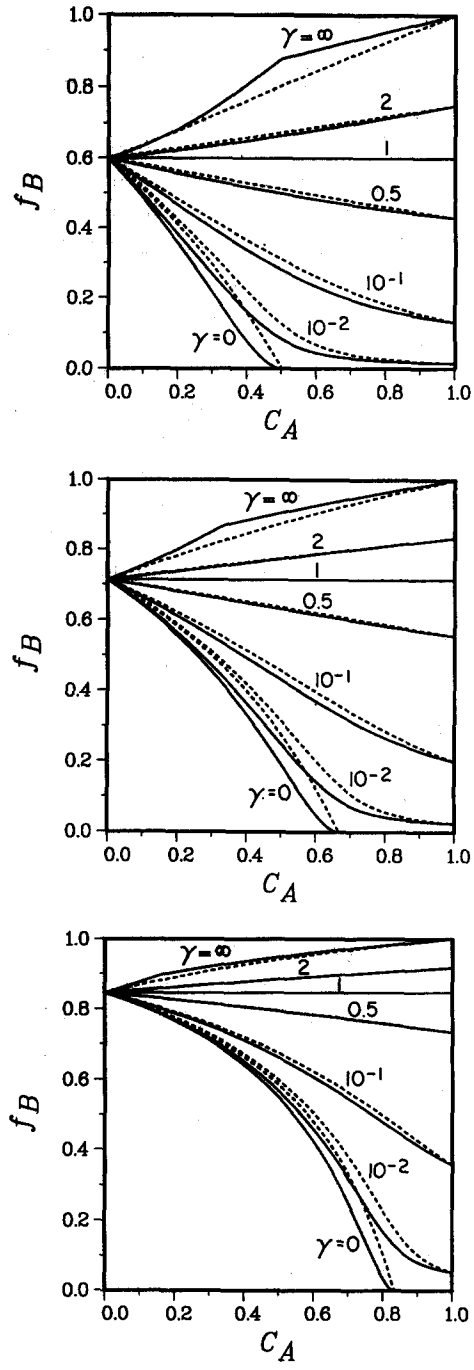

FIG. 6. The correlation factor f_B ($= D_{tB}/c_V$) in the small vacancy concentration limit ($c_V \to 0$) for three different lattices: square [Fig. 6(a)], simple cubic [Fig. 6(b)] and face centered cubic [Fig. 6(c)]. The results are solutions to Eq. (6.4) with $\Gamma_0 = \Gamma_B$ using the EMA threshold $p_c = 2/Z$ and Eqs. (7.11) (full lines) and (4.1) (dashed lines) for τ_A and τ_B ($\omega = 0$ in all cases).

static percolation behavior for $c_A < 1 - p_c$ to motion dominated by the A dynamics for $c_A > 1 - p_c$. Obviously, for concentrations $c_B > p_c$ ($c_B = 0.5, 0.7$) no such a crossover behavior is seen (since D_{tB} vanishes for $c = 1$), and the difference between these and the static A results is relatively small.

Figures 6(a)–6(c) display the correlation factor f_B ($= D_{tB}/c_V$) in the small vacancy concentration limit ($c_V \to 0$) for three different lattices: square, simple cubic, and face centered cubic, respectively. f_B is found by solving Eq. (6.4) with $\Gamma_0 = \Gamma_B$. The results for different ratios $\gamma = \Gamma_A/\Gamma_B$ are plotted against c_A. In these figures full lines represent results obtained using choice (i) for τ_A and τ_B while dashed lines correspond to choice (ii). A common feature to these results is that both choices for τ_A and τ_B yield almost identical results for intermediate values of $\gamma (0.1 < \gamma < 10)$ while significant differences are seen for $\gamma \to 0, \infty$.

Sato and Kikuchi[25] have presented two different theoretical calculations for the tracer diffusion coefficient in a binary NILG model similar to the one under discussion and for the small vacancy concentration limit. For $\gamma \to 0$ our theory (for f_B) agrees rather well with their latter improved theory, except for details associated with the percolation threshold. The percolation threshold obtained by Sato and Kikuchi is that of the Bethe lattice $p_c = 1/(Z-1)$ and, for realistic dimensions, is worse than the EMA result $p_c = 2/Z$ (for most lattices). Their theory predicts a linear (in $1 - c_A - p_c$) approach to the threshold, the same result as obtained for choice (ii) (for τ_B) in the present theory. The expression obtained from their theory for this limit may be written as $f_B = (1 - c_A - p_c)/(1 - c_A + p_c)$, and is quantitatively different from our result Eq. (6.5) even when the same value for p_c and the mean-field approximation for τ_B, choice (ii) [Eq. (6.1b)], are being used. In the opposite limit $\gamma \to \infty$, the major disagreement (with their improved theory) discussed above [following Eq. (6.6)] is seen. It is interesting to note that some similarity (showing the hump in the $\gamma \to \infty$ line) exists between the Sato–Kikuchi results and our results using choice (i) for τ_A and τ_B. On the other hand, a very good quantitative agreement exists in this limit ($\gamma \to \infty$) between our results in Figs. 6(a)–6(c) and the original theory of Sato and Kikuchi,[25] when the mean-field choice (ii) is made for τ_B. This agreement exists in the whole concentration range. We note again that the simulation results in the dynamical regime $\gamma \gg 1$ shown in Fig. 4, seem to agree with our theoretical predictions [especially those obtained from choice (ii)] and with the original theory of Sato and Kikuchi.[25]

TABLE II. Tracer diffusion correlation factors f_A and f_B for a three-dimensional, simple cubic lattice for the case $\gamma = \Gamma_A/\Gamma_B = 10$ and $c_A = c_B$. Equations (7.11) were used for the fluctuation times τ_A and τ_B. The results of using Eqs. (4.1) for these times differ by less than 1%.

c_A	f_A [a]	f_A [b]	f_A [c]	f_B [a]	f_B [b]	f_B [c]
0.100	0.928	0.934	0.920 ± 0.01	0.975	0.977	0.966 ± 0.015
0.150	0.884	0.894	0.865 ± 0.003	0.962	0.964	0.950 ± 0.005
0.200	0.835	0.848	0.807 ± 0.003	0.948	0.952	0.931 ± 0.005
0.250	0.780	0.796	0.746 ± 0.0025	0.935	0.939	0.915 ± 0.004
0.300	0.718	0.738	0.675 ± 0.002	0.921	0.926	0.895 ± 0.004
0.350	0.650	0.672	0.598 ± 0.002	0.907	0.913	0.874 ± 0.004
0.400	0.578	0.601	0.522 ± 0.002	0.893	0.900	0.851 ± 0.004
0.450	0.504	0.528	0.453 ± 0.002	0.879	0.886	0.859 ± 0.004
0.475	0.467	0.490	0.400 ± 0.01	0.871	0.879	0.830 ± 0.015

[a] From Eqs. (3.9) using the EMA p_c, $p_c = 0.3333$.
[b] From Eqs. (3.9) using the exact p_c, $p_c = 0.3117$.
[c] Simulation results from Ref. 28.

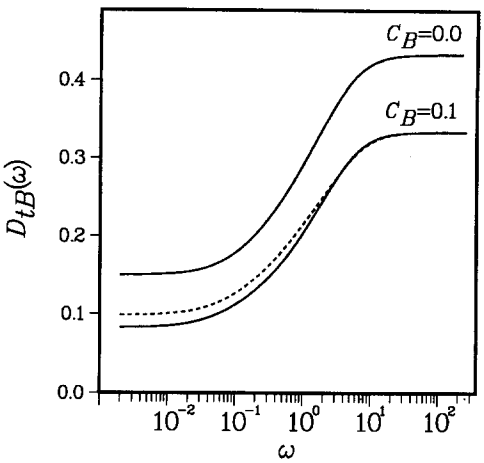

FIG. 7. Tracer diffusion coefficient D_{tB} (real part) plotted against the frequency ω (SC lattice) for the static A background case, with concentration $c_A = 1 - p_c - 0.1 \simeq 0.567$, for $c_B = 0$ (single particle diffusion) and $c_B = 0.1$. The results are solutions to Eq. (3.9), with $\Gamma_0 = \Gamma_B$, $\lambda_+ = (1 - c_A)\tau_B^{-1}$ and $\lambda_- = 0$, using Eqs. (5.4a) (dashed line) and (5.5) (full line) for τ_B.

In Table II we compare our theoretical results to the simulation results of El-Meshad Tahir-Kheli[28] for a SC lattice. Our theory is expected to work better for lattices with larger coordination number Z. Indeed the good agreement [for both choices (i) and (ii)] is encouraging. We note that the theory of El-Meshad and Tahir-Kheli[28] also works fairly well for this case but is poor in the $\gamma \to 0$ limit, unable to predict the percolation threshold.

Finally, in Fig. 7 we show the frequency dependence of the real part of the diffusion coefficient D_{tB} of a tracer B particle ($\Gamma_0 = \Gamma_B$) in a static A background (as in Figs. 1–3) of concentration $1 - c_A - p_c = 0.1$, for $c_B = 0$ and for $c_B = 0.1$. The results shown are for a SC lattice. They are obtained by solving Eq. (3.9) with $\lambda_+ = (1 - c_A)\tau_B^{-1}$ [as given in (5.1a)] while λ_- is set to zero [for the reasons explained after Eq. (5.2)], namely, $\epsilon_- = i\omega/\psi$. Unlike in the calculation described above, where the exact lattice Green's functions where used, we have used here the approximate expression Eq. (E8). The solid line again represents the use of choice (i) for τ_B, and the dashed line corresponds to choice (ii). It is seen (for both choices) that the gap in the diffusion coefficient between the $\omega = 0$ and $\omega \to \infty$ limits decreases as the concentration of the moving particles c_B increases. The qualitative form of the curves is however similar for both $c_B = 0$ and $c_B = 0.1$ (and for both choices for τ_B).

IX. CONCLUSIONS

In this paper we applied dynamic percolation theory to develop an effective medium approximation for the diffusion of mixtures of particles with hard core interactions. The resulting EMA expression for the tracer diffusion coefficient is expressed in terms of relaxation times for local concentration fluctuations in the vicinity of the tracer. The latter are expressed in terms of the chemical diffusion coefficients of the system; however, simpler mean-field expressions also work quite well. A recent treatment[47] in the DBP framework of a noninteracting lattice gas in a static percolating *bond* network (where the particle concentration is not limited by the absent bonds concentration) yields similar results.

Results of this theory were shown to work well when single bond dynamics and (single bond) effective medium approximation hold. In other situations a considerable improvement is obtained if the exact concentration at the percolation threshold replaces the EMA value in the EMA expression for the tracer diffusion coefficient. The method advanced here can be improved in a more consistent way by using many bond EMAs[38] (cluster EMAs) to include correlations that exist in the bond network. "Static" correlations are a result of the site randomness property while "dynamic" correlations exist between occupation–deoccupation events in nearest-neighbor sites. An example of partially incorporating the dynamical correlations is already described in Ref. 16. Taking into account the static correlation can help to avoid the necessity for an artificial replacement of the EMA percolation threshold by the actual site percolation threshold.

The present work was limited to hard core interactions (double site occupancy excluded). Longer range interactions have to be included in order to discuss realistic systems. A dynamic percolation theory approach, which accommodates long range interactions, was described in a previous paper[16] and further work along this line is proceeding.

ACKNOWLEDGMENTS

This work was supported in part by the US-Israel Binational Science Foundation. We thank Mark A. Ratner and Steve D. Druger for many useful discussions and Marvin Silverberg for many useful discussions and for the use of his computer programs for lattice diffusion of interacting particles. R. G. thanks Professor Mark Ratner for his hospitality during a period when part of this work was done.

APPENDIX A

Here we repeat our derivation of Eqs. (2.7) and (2.8), previously described in Ref. 38 for the case of stochastic hopping rates which explicitly depend on time, generalizing it to the case of hopping rates which depend on time via another (stochastic) physical quantity, e.g., the instantaneous local configuration. In the HZ formalism,[37] which is the basis of the present work, one starts by writing Eq. (2.5) for the walker probability $P_i(t)$ to be at site i at time t, in the vector form

$$\frac{d}{dt}\mathbf{P} = -\mathbf{W}\cdot\mathbf{P} \equiv -\sum_{\alpha} \sigma(\xi_\alpha(t))\mathbf{V}_\alpha \cdot \mathbf{P}, \tag{A1}$$

where α corresponds to a bond (ij) between the nearest-neighbor sites i and j,

$$\mathbf{V}_\alpha = \mathbf{S}_\alpha \mathbf{S}_\alpha \dagger = (|i\rangle - |j\rangle)(\langle i| - \langle j|), \tag{A2a}$$

$$\mathbf{P} = \sum_i P_i |i\rangle, \tag{A2b}$$

and where the bond state variable ξ_α can take the symbolic values $A_1, A_2, \ldots, A_n, V$. The bond dynamics between the

different states is described by [c.f., Eq. (2.2)]

$$\frac{\partial}{\partial t}f_\alpha(\xi_\alpha,t)=\sum_{\xi'}\Omega_\alpha(\xi_\alpha,\xi'_\alpha)f_\alpha(\xi'_\alpha,t)\equiv\hat{\Omega}f_\alpha(\xi_\alpha,t). \tag{A3}$$

The joint probability distribution $f(\mathbf{P},\xi,t)$ to find the walker distributed according to $\mathbf{P}$ and the bonds in the collective state $\xi=(\xi_1,\xi_2,...,\xi_\alpha,...)$ at time t, satisfies the Liouville master equation

$$\frac{\partial}{\partial t}f=\frac{\partial}{\partial \mathbf{P}}\cdot(\mathbf{W}\cdot\mathbf{P}f)+\hat{\Omega}f, \tag{A4}$$

where, since all the bonds fluctuate independently,

$$\hat{\Omega}=\sum_\alpha\hat{\Omega}_\alpha. \tag{A5}$$

For the initial condition we take

$$f(\mathbf{P},\xi,t=0)=\delta(\mathbf{P}-\mathbf{P}_0)\rho(\xi), \tag{A6}$$

where $\rho(\xi)$ is the equilibrium distribution for the collective bond state, namely,

$$\rho(\xi)=\prod_\alpha\rho_\alpha(\xi_\alpha), \tag{A7}$$

$$\hat{\Omega}_\alpha\rho(\xi_\alpha)\equiv\sum_{\xi'}\Omega_\alpha(\xi_\alpha,\xi'_\alpha)\rho_\alpha(\xi'_\alpha)=0 \tag{A8}$$

and where $\mathbf{P}_0$ is an arbitrary vector in site space. In order to get an equation of the type (2.6), let us follow the evolution in time of the average of $\mathbf{P}$. The partial average of $\mathbf{P}$ is given by

$$\mathbf{P}(\xi,t)=\int d\mathbf{P}\,\mathbf{P}f(\mathbf{P},\xi,t). \tag{A9}$$

The full average of $\mathbf{P}$ is just $\Sigma_\xi\mathbf{P}(\xi,t)$. Using Eq. (A4) and integration by parts, $\mathbf{P}(\xi,t)$ is shown to satisfy

$$\frac{\partial}{\partial t}\mathbf{P}(\xi,t)=-\mathbf{W}\cdot\mathbf{P}(\xi,t)+\hat{\Omega}\mathbf{P}(\xi,t) \tag{A10}$$

with the initial condition [using Eqs. (A6) and (A9)]

$$\mathbf{P}(\xi,t=0)=\mathbf{P}_0\rho(\xi). \tag{A11}$$

Taking the Fourier–Laplace transform

$$\mathbf{P}(\xi,i\omega)=\lim_{\epsilon\to0}\int_0^\infty dt\,e^{-i\omega t-\epsilon t}\mathbf{P}(\xi,t) \tag{A12}$$

of Eq. (A10) leads to

$$\mathbf{P}(\xi,i\omega)=\mathbf{g}(\xi,i\omega)\cdot\mathbf{P}_0 \tag{A13}$$

with the partially averaged Green's operator formally given by

$$\mathbf{g}(\xi,i\omega)=[(i\omega-\hat{\Omega})\mathbf{1}+\mathbf{W}(\xi)]^{-1}\rho(\xi). \tag{A14}$$

The fully averaged Green's operator $\mathbf{g}(\omega)$, corresponding to the full average of $\mathbf{P}$

$$\langle\mathbf{P}(\omega)\rangle=\sum_\xi\mathbf{P}(\xi,i\omega)\equiv\mathbf{g}(\omega)\mathbf{P}_0, \tag{A15}$$

is

$$\mathbf{g}(\omega)=\sum_\xi\mathbf{g}(\xi,i\omega)\equiv[i\omega\mathbf{1}+\mathbf{W}_m(\omega)]^{-1}, \tag{A16}$$

where

$$\mathbf{W}_m(\omega)=\psi(\omega)\sum_\alpha\mathbf{V}_\alpha, \tag{A16a}$$

which defines the frequency-dependent complex effective medium rate $\psi(\omega)$. In the time domain, Eqs. (A15)–(A16) lead to Eq. (2.6).

In the (single bond) EMA one considers one fluctuating bond (bond 1) in an otherwise effective environment with bond rates $\psi(\omega)$. The latter is obtained self-consistently by writing

$$\mathbf{W}=\psi(\omega)\sum_{\alpha\neq1}\mathbf{V}_\alpha+\sigma(\xi_1)\mathbf{V}_1$$

$$=\mathbf{W}_m+[\sigma(\xi_1)-\psi(\omega)]\mathbf{V}_1, \tag{A17a}$$

$$\hat{\Omega}=\hat{\Omega}_1. \tag{A17b}$$

By Eqs. (A13) and (A15), the effective medium rate is determined from the condition

$$[i\omega\mathbf{1}+\mathbf{W}_m(\omega)]^{-1}=\sum_{\xi_1}\Gamma_{\xi_1} \tag{A18}$$

with

$$\Gamma_{\xi_1}=\{(i\omega-\hat{\Omega}_1)\mathbf{1}+\mathbf{W}_m+[\sigma(\xi_1)-\psi]\mathbf{V}_1\}^{-1}\rho_1(\xi_1). \tag{A19}$$

Note that Eq. (A18) implies that the site space operators Γ_{ξ_1} cannot all be equal to zero. In the following we shall make use of this fact. Suppressing the bond index 1, one can write Eq. (A19) as

$$\{i\omega\mathbf{1}+\mathbf{W}_m+[\sigma(\xi)-\psi]\mathbf{V}\}\Gamma_\xi$$

$$-\sum_{\xi'}\Omega(\xi,\xi')\Gamma_{\xi'}=\rho(\xi)\mathbf{1}. \tag{A20}$$

Multiplying Eq. (A20) with the elements $M_\xi^{(l)}$ of the left eigenvector of the operator $\hat{\Omega}(=\hat{\Omega}_1)$,

$$\sum_{\xi'}M_{\xi'}^{(l)}\Omega(\xi',\xi)=-\lambda_l M_\xi^{(l)},\quad \lambda_l\geq0, \tag{A21}$$

yields

$$\sum_\xi[\sigma(\xi)-\psi]\mathbf{V}\cdot\Gamma_\xi=0, \tag{A22}$$

from the $\lambda_0=0$ case, and

$$\sum_\xi M_\xi^{(l)}[(i\omega+\lambda_l)\mathbf{1}+\mathbf{W}_m$$

$$+[\sigma(\xi)-\psi]\mathbf{V}]\cdot\Gamma_\xi=0\quad l=1,...,n \tag{A23}$$

for $\lambda_l\neq0$, where, in addition to Eqs. (A21) and (A18), we have used the fact that one eigenvalue [with the eigenvector $(1,1,...,1)$] is zero, and also the orthogonality relation between left and right eigenvectors of different eigenvalues. Equation (A22) is identical to Eq. (2.7) (when multiplied by $\mathbf{S}\dagger\equiv\mathbf{S}_1\dagger$ and defining $\mathbf{Q}_\xi=\mathbf{S}\dagger\cdot\Gamma_\xi$). Multiplying Eq. (A23) from the left by $\mathbf{S}\dagger\cdot\mathbf{H}^{(l)}$ where

$$\mathbf{H}^{(l)}=[(i\omega+\lambda_l)\mathbf{1}+\mathbf{W}_m]^{-1} \tag{A24}$$

then leads to Eq. (2.8) (see Ref. 38 for more details).

APPENDIX B

Here we dwell on the limiting value of

$$F_-=\frac{c_V-\tau_A\lambda_-}{c_V-\tau_B\lambda_-} \tag{B1}$$

(mentioned in Sec. III) for the case $\tau_A\to\tau_B$. Although the

exact value of F_- does not influence the fact that $\psi(\omega)$ reduces for this limit to its single component form Eq. (3.10) (as long as $1-F_-$ is nonzero), it does however determine the asymptotic behavior of $\psi(\omega)$ when $\tau_A \simeq \tau_B$.

Suppose that, to the first order in $\delta\tau$,

$$\tau_B \simeq \tau + \delta\tau \tag{B2a}$$

and

$$\tau_A \simeq \tau - k\delta\tau, \tag{B2b}$$

where k is a constant different from -1. Using Eq. (3.2) we have, to the first order in $\delta\tau$,

$$\lambda_- \simeq \lambda^0_- + \lambda^1_- \delta\tau \tag{B3}$$

where

$$\lambda^0_- = \frac{c_V}{\tau}, \tag{B4a}$$

$$\lambda^1_- = -\frac{(c_A - kc_B)c_V}{c\tau^2}, \tag{B4b}$$

and, in the limit $\delta\tau \to 0$, F_- becomes

$$F_- = \frac{\lambda^1_- \tau - k\lambda^0_-}{\lambda^1_- \tau + \lambda^0_-} = -\frac{c_A}{c_B}. \tag{B5}$$

APPENDIX C

Here we rederive and summarize some important results related to the Onsager and the chemical diffusion coefficients in the n component NILG model. We start by deriving the generalized Einstein relations that relates the Onsager coefficients to the chemical diffusion coefficients. For brevity, we shall adopt an n component version, instead of the $n+1$ component version which is more common in the literature,[17,24] where vacancies are considered at first as independent particles. The final results are of course the same in both versions.

Consider first the n component NILG with $\{N_i\}$ $i = 1, \ldots, n$ being the number of particles of the different components, and N_0 being the total number of sites in the lattice. The Helmholtz free energy of the ideal mixture is readily obtained (up to a constant) as

$$F = k_B T\left(\sum_i N_i \ln N_i + N_V \ln N_V - N_0 \ln N_0\right), \tag{C1}$$

$$N_V = N_0 - N = N_0 - \sum_i N_i, \tag{C1a}$$

where N_V is the number of vacancies and N is the total number of particles. The chemical potentials $\{\mu_i\}$ are defined as

$$\mu_i = \left(\frac{\partial F}{\partial N_i}\right)_{T, N_{j(\neq i)}}. \tag{C2}$$

In the n component version, in contradiction to the $n+1$ component version, one uses explicitly the constraint (C1a) in the derivation of the chemical potentials. Thus, we find

$$\mu_i = k_B T \ln\left(\frac{c_i}{c_V}\right), \quad i = 1, \ldots, n, \tag{C3}$$

where $c_V = 1 - c = 1 - \Sigma_i c_i$. From this result one obtains

$$\left(\frac{\partial \mu_i}{\partial c_j}\right)_{T, c_{k(\neq j)}} = k_B T\left(\frac{\delta_{ij}}{c_i} + \frac{1}{c_V}\right). \tag{C4}$$

In the linear regime and in an isothermal system ($\nabla T = 0$), the fluxes $\mathbf{J}_i$ are related to the gradients of the chemical potential (the thermodynamic forces) by[24,47]

$$\mathbf{J}_i = -\beta \sum_{j=1}^{n} \Lambda_{ij} (\nabla \mu_j)_T, \tag{C5}$$

where $\beta = (k_B T)^{-1}$. The Onsager coefficients Λ_{ij} obey the Onsager reciprocal relations[48]

$$\Lambda_{ij} = \Lambda_{ji}. \tag{C6}$$

Assuming now local equilibrium, namely, $\mu_i(\mathbf{x}) = \mu_i(\{c_j(\mathbf{x})\})$ ($\mathbf{x}$ is the position vector) with $\mu_i(\{c_j\})$ being the equilibrium expressions for the chemical potentials, one finds the generalized Fick's law

$$\mathbf{J}_i = -\sum_{k=1}^{n} D_{ik} \nabla c_k \tag{C7a}$$

with the chemical diffusion coefficients D_{ik} related to the Onsager coefficients Λ_{ij} by the generalized Einstein relations

$$D_{ik} = \beta \sum_j \Lambda_{ij} \left(\frac{\partial \mu_j}{\partial c_k}\right)_{T, c_{l(\neq k)}}. \tag{C7b}$$

Together with the continuity equations

$$\frac{\partial c_i}{\partial t} + \nabla \cdot \mathbf{j}_i = 0 \tag{C8}$$

Eq. (C5) leads (for small gradients) to n coupled diffusion equations

$$\frac{\partial c_i}{\partial t} = \sum_{j=1}^{n} D_{ij} \nabla^2 c_j. \tag{C9}$$

Using now Eq. (C4) for the NILG case we finally obtain from Eq. (C7b)

$$D_{ik} = \frac{\Lambda_{ik}}{c_k} + \frac{1}{c_V} \sum_{j=1}^{n} \Lambda_{ij}. \tag{C10}$$

With the symmetry relations Eq. (C6), only $n(n+1)/2$ Onsager or chemical diffusion coefficients are independent. For the NILG case, the number of independent coefficients is further reduced to only $n(n-1)/2$ by the recently established[26(a)] exact relations between the Onsager coefficients, which, in our units (lattice constant $a = 1$), read

$$\sum_i \frac{\Lambda_{ij}}{\Gamma_i} = c_j c_V, \quad j = 1, \ldots, n. \tag{C11}$$

For the NILG binary mixture ($n = 2$) we have from Eq. (C10)

$$D_{AA} = \Lambda_{AA} \frac{1 - c_B}{c_A c_V} + \frac{\Lambda_{AB}}{c_V}, \tag{C12a}$$

$$D_{AB} = \frac{\Lambda_{AA}}{c_V} + \Lambda_{AB} \frac{1 - c_A}{c_B c_V}, \tag{C12b}$$

$$D_{BA} = \Lambda_{AB} \frac{1 - c_B}{c_A c_V} + \frac{\Lambda_{BB}}{c_V}, \tag{C12c}$$

$$D_{BB} = \frac{\Lambda_{AB}}{c_V} + \Lambda_{BB} \frac{1 - c_A}{c_B c_V}, \tag{C12d}$$

where use was made of the Onsager symmetry relation

$\Lambda_{AB} = \Lambda_{BA}$. In addition, Eqs. (C11) become in this case (using again $\Lambda_{AB} = \Lambda_{BA}$)

$$\frac{\Lambda_{AA}}{\Gamma_A} + \frac{\Lambda_{AB}}{\Gamma_B} = c_A c_V, \tag{C13a}$$

$$\frac{\Lambda_{AB}}{\Gamma_A} + \frac{\Lambda_{BB}}{\Gamma_B} = c_B c_V, \tag{C13b}$$

so that only one (diffusion or Onsager) coefficient is independent. These relations were found to compare well with recent numerical simulations.[17]

APPENDIX D

In this appendix we obtain an exact result for the chemical diffusion coefficient of a single component NILG in a *dynamically disordered* lattice. This exact result is used in Sec. VII as an ansatz for obtaining the chemical diffusion coefficients in a binary mixture and in an ordered lattice. Following the proof of Kutner[14(a)] for an ordered lattice, the occupation dynamics of a single component NILG in a dynamically disordered lattice in described exactly by

$$\frac{d}{dt}P(l,t) = \sum_{l'} \sigma_{ll'}(t)[P(l',\bar{l},t) - P(l,\bar{l}',t)], \tag{D1}$$

where $P(l,t)$ is the occupation probability of the lattice site l at time t, $P(l',\bar{l},t)$ is the joint probability to have the site l' occupied by a particle and site l vacant and $\sigma_{ll'}(t)$ is the stochastic bond hopping rate [hence $P(l,t)$ and $P(l',\bar{l},t)$ are also stochastic]. Now for any specific path of the transition rates $\{\sigma_{ll'}(t)\}$ (out of the ensemble of paths) and for any pair of sites l and l' we have

$$P(l',\bar{l},t) + P(l',l,t) = P(l',t), \tag{D2a}$$

$$P(l,\bar{l}',t) + P(l,l',t) = P(l,t), \tag{D2b}$$

where $P(l',l,t) \equiv P(l,l',t)$ is the joint probability to have both sites l and l' occupied. With Eqs. (D2a) and (D2b), Eq. (D1) is identical to the "single particle" equation

$$\frac{d}{dt}P(l,t) = \sum_{l'} \sigma_{ll'}(t)[P(l',t) - P(l,t)]. \tag{D3}$$

Thus, the chemical diffusion coefficient of this lattice gas, which is found by averaging over Eq. (D3), is identical to the single particle diffusion coefficient on the same dynamically disordered lattice.

APPENDIX E

Here we summarize some expressions for the lattice Green's function $g(\epsilon)$ for the square, simple cubic, and face-centered-cubic lattices, used in the numerical solutions described in Secs. VII and VIII. For a square lattice[6]

$$g(\epsilon) = \frac{1}{2}\int_0^\infty dt \exp(-2t - \tfrac{1}{2}\epsilon t) I_0^2(t)$$

$$= \frac{1}{2\pi}(1+\epsilon/4)^{-1} K([1+\epsilon/4]^{-1}), \tag{E1}$$

where $I_m(t)$ is the modified Bessel function of order m, and where $K(k)$ is the complete elliptic integral of the first kind

$$K(k) = \int_0^{\pi/2} \frac{d\theta}{\sqrt{1-k^2\sin^2\theta}}. \tag{E2}$$

For the simple cubic lattice

$$g(\epsilon) = \frac{1}{2}\int_0^\infty dt \exp(-3t - \tfrac{1}{2}\epsilon t) I_0^3(t) \tag{E3}$$

or[49]

$$g(\epsilon) = \tfrac{1}{2}F(3+\epsilon/2), \tag{E4}$$

where

$$F(u) = (8/\pi^2 u)\left\{\frac{(\zeta+1)(\zeta+4)}{\zeta^2+8\zeta+8+4(2+\zeta)(\zeta+1)^{1/2}}\right\}^{1/2} \times K(k_+)K(k_-) \tag{E5}$$

with

$$k_\pm^2 = \frac{\zeta[(\zeta+1)^{1/2} \pm (\zeta+4)^{1/2}] - 2[1-(\zeta+1)^{1/2}]}{\zeta[(\zeta+1)^{1/2} \pm (\zeta+4)^{1/2}] + 2[1+(\zeta+1)^{1/2}]} \tag{E6}$$

and

$$\zeta = \frac{u^2+3-[(u^2-9)(u^2-1)]^{1/2}}{u^2-3+[(u^2-9)(u^2-1)]^{1/2}}, \quad u \geqslant 3. \tag{E7}$$

A useful approximate expression is given by Odagaki and Lax[3]

$$g(\epsilon) = 2\{\epsilon+6+[\epsilon(\epsilon+12)]^{1/2}\}^{-1}. \tag{E8}$$

For an fcc lattice[49]

$$g(\epsilon) = \tfrac{1}{4}G(3+\epsilon/4), \tag{E9}$$

where

$$G(u) = (4/\pi^2)(u+1)^{-1}K(k_+)K(k_-) \tag{E10}$$

with

$$k_\pm^2 = (u+1)^{-2}\left[\tfrac{1}{16}\{(u+1)^{1/2} - (u-3)^{1/2}\}^4 + \{(u+1)^{1/2} \pm u^{1/2}\}^2\right], \quad u \geqslant 3. \tag{E11}$$

[1] D. Stauffer, *Introduction to Percolation Theory* (Taylor & Francis, London, 1985).
[2] S. Havlin and D. Ben-Avraham, Adv. Phys. **36**, 695 (1987).
[3] T. Odagaki and M. Lax, Phys. Rev. B **24**, 5284 (1981).
[4] I. Webman, Phys. Rev. Lett. **47**, 1496 (1981).
[5] S. Summerfield, Solid State Commun. **39**, 401 (1981).
[6] M. Sahimi, B. D. Hughes, L. E. Scriven, and H. T. Davis, J. Chem. Phys. **78**, 6849 (1983).
[7] Y. Gefen, A. Aharony, and S. Alexander, Phys. Rev. Lett. **50**, 77 (1983).
[8] (a) C. P. Flynn, *Point Defects and Diffusion* (Clarendon, Oxford, 1972); A. R. Allnatt and A. B. Lidiard, Rep. Prog. Phys. **50**, 373 (1987). (b) D. E. Day, J. Non-Cryst. Solids **21**, 343 (1976); G. V. Chandrashekhar and L. M. Foster, Solid State Commun. **27**, 169 (1978); J. A. Bruce, C. C. Hunter, and M. D. Ingram, Solid State Ionics **28–30**, 306 (1988). (c) G. Ehrlich and K. Stolt, Ann. Rev. Phys. Chem. **31**, 603 (1980); S. C. Wang and R. Gomer, J. Chem. Phys. **83**, 4193 (1985); M. V. Rama Krishna and K. B. Whaley (to be published). (d) K. Binder and H. Sillescu, in *Encyclopedia of Polymer Science and Engineering*, 2nd ed., edited by J. L. Kroschwitz (Wiley, New York, in press).
[9] (a) J. Bardeen and C. Herring, in *Imperfections in Nearly Perfect Crystals*, edited by W. Shockley (Wiley, New York, 1952), p. 261. (b) J. R. Manning, *Diffusion Kinetics for Atoms in Crystals* (Van Nostrand, Princeton, N. J., 1968).
[10] R. Kikuchi, Prog. Theor. Phys. Suppl. **35**, 1 (1966).
[11] G. L. Montet, Phys. Rev. B **7**, 650 (1973).
[12] O. F. Sankey and P. A. Fedders, Phys. Rev. B **15**, 3586 (1977).
[13] K. Nakazato and K. Kitahara, Prog. Theor. Phys. **64**, 2261 (1980).
[14] (a) R. Kutner, Phys. Lett. **81A**, 239 (1981). (b) K. W. Kehr, R. Kutner, and K. Binder, Phys. Rev. B **23**, 4931 (1981), and references therein. (c) R. Kutner and K. W. Kehr, Philos. Mag. A **48**, 199 (1983). (d) K. W.

Kehr and K. Binder, in *Applications of the Monte Carlo Method in Statistical Physics*, edited by K. Binder (Springer, New York, 1987), p. 181.
[15] R. A. Tahir-Kheli, Phys. Rev. B **35**, 5503 (1987).
[16] R. Granek and A. Nitzan, J. Chem. Phys. **92**, 1329 (1990).
[17] K. W. Kehr, K. Binder, and S. M. Reulein, Phys. Rev. B **39**, 4891 (1989).
[18] A. R. Allnatt and E. L. Allnatt, Phil. Mag. A **49**, 625 (1984).
[19] M. Braun and K. W. Kehr, Philos. Mag. A **61**, 855 (1990).
[20] L. Heupel, J. Stat. Phys. **42**, 541 (1986).
[21] G. E. Murch, *Atomic Diffusion Theory in Highly Defective Solids* (Trans Tech SA, Aedermannsdorf, 1980).
[22] C. H. Mark, H. C. Andersen, and S. M. George, J. Chem. Phys. **88**, 4052 (1988).
[23] H. Harder, A. Bunde, and W. Dieterich, J. Chem. Phys. **85**, 4123 (1986).
[24] E. Howard and A. B. Lidiard, Rep. Prog. Phys. **27**, 161 (1964).
[25] H. Sato and R. Kikuchi, Phys. Rev. B **28**, 648 (1983).
[26] (a) L. K. Moleko and A. R. Allnatt, Philos. Mag. A **58**, 677 (1988), and references therein. (b) L. K. Moleko, Y. Okamura, and A. R. Allnatt, J. Chem. Phys. **88**, 2706 (1988).
[27] J. R. Manning, Phys. Rev. B **4**, 1111 (1971).
[28] N. El- Meshad and R. A. Tahir-Kheli, Phys. Rev. B **32**, 6176 (1985).
[29] S. D. Druger, A. Nitzan, and M. A. Ratner, J. Chem. Phys. **79**, 3133 (1983).
[30] S. D. Druger, M. A. Ratner, and A. Nitzan, Solid State Ionics **9/10**, 1115 (1983).
[31] S. D. Druger, M. A. Ratner, and A. Nitzan, Phys. Rev. B **31**, 3939 (1985).
[32] S. D. Druger, in *Transport and Relaxation Processes in Random Materials*, edited by J. Klafter, R. J. Rubin, and M. F. Shlesinger (World Scientific, Singapore, 1986).
[33] A. Nitzan, S. D. Druger, and M. A. Ratner, Philos. Mag. B **56**, 853 (1987).
[34] R. Granek, A. Nitzan, S. D. Druger, and M. A. Ratner, Solid State Ionics **28–30**, 120 (1988).
[35] S. D. Druger and M. A. Ratner, Chem. Phys. Lett. **151**, 434 (1988).
[36] S. D. Druger and M. A. Ratner, Phys. Rev. B **38**, 12,589 (1988).
[37] A. K. Harrison and R. Zwanzig, Phys. Rev. A **32**, 1072 (1985); denoted by HZ in the paper.
[38] R. Granek and A. Nitzan, J. Chem. Phys. **90**, 3784 (1989).
[39] G. S. Grest, I. Webman, S. A. Safran, and A. L. R. Bug, Phys. Rev. A **33**, 2842 (1986).
[40] A. R. Kerstein and B. F. Edwards, Phys. Rev. B **33**, 3353 (1986).
[41] A. L. R. Bug and Y. Gefen, Phys. Rev. A **35**, 1301 (1985).
[42] (a) R. Hilfer and R. Orbach, Chem. Phys. **128**, 275 (1988). (b) R. Hilfer and R. Orbach, in *Dynamical Processes in Condensed Molecular Systems*, edited by J. Klafter, J. Jortner, and A. Blumen (World Scientific, Singapore, 1989), p. 175.
[43] To prove this identity we have used the REDUCE symbol manipulation program.
[44] The problem may be also held to the discretization procedure described here.
[45] We thank H. Sato for raising up this point.
[46] Both calculations overestimate the resulting D_{tB} for small c_A. This results mainly from the neglect of correlations in the occupation dynamics as discussed in Ref. 16.
[47] M. Silverberg, M. A. Ratner, R. Granek, and A. Nitzan, J. Chem. Phys. **93**, 3420 (1990).
[48] S. R. De Groot and P. Mazur, *Non-Equilibrium Thermodynamics* (North-Holland, Amsterdam, 1969).
[49] M. L. Glaser and I. J. Zucker, Proc. Natl. Acad. Sci. USA **74**, 1800 (1977); note that there is a missing power 2 for the second curely brackets in Eq. (3a), corrected in Eq. (E11) in this paper.